Title:

Genetic risk in endolysosomal network genes correlates with endolysosomal dysfunction across neural cell types in Alzheimer's disease

Mamde S*[1], Rose SE*[2], Prater KE*[3], Cochoit A[3], Lin YF[4], Smith I[3], Johnson CS[3], Reid AN[3], Qiu W[4], Strohbehn S[5], Keene CD[2], Rolf BA[5], Lin KZ[6], Lee SI[4], Garden GA[7], Blue EE[5], Young JE[#2,8], Jayadev S[#3,5,8]

1. Department of Cellular and Molecular Medicine, University of California San Diego, San Diego, CA
2. Department of Laboratory Medicine and Pathology, University of Washington, Seattle WA
3. Department of Neurology, University of Washington, Seattle WA
4. Paul G Allen School of Computer Science and Engineering, University of Washington, Seattle WA
5. Department of Medicine, Division Medical Genetics, University of Washington, Seattle WA
6. Department of Biostatistics, School of Public Health, University of Washington, Seattle WA
7. Department of Neurology, University of North Carolina, Chapell Hill, NC
8. Institute of Stem Cell and Regenerative Medicine, University of Washington, Seattle WA

***** authors contributed equally to this work
# co-corresponding authors

Correspondence:
Jessica Young PhD: jeyoung@uw.edu
Suman Jayadev MD: sumie@uw.edu

Running Title: Cell-type specific molecular and functional effects of AD risk variants

Funding Sources:
NIA: UW Alzheimer Disease Training Program T32
NIA: P30 AG066509 UW Alzheimer Disease Research Center
NIA: R01AG080585, RF1AG063540

Acknowledgements: We are grateful to study participants and their families for making the most generous of donation, their brain for research.

The authors have nothing to declare

ABSTRACT

Late-onset Alzheimer's disease (LOAD) has a complex genomic architecture with risk variants in multiple pathways, including the endolysosomal network (ELN). Whether genetic risk in specific pathways correlates with corresponding biological dysfunction remains largely unknown. We developed an endolysosomal pathway-specific polygenic risk score (ePRS) using 13 established AD GWAS loci containing ELN genes. We investigated the association between ePRS and AD neuropathology, then examined cell-specific endolysosomal morphology and transcriptomic profiles in post-mortem dorsolateral prefrontal cortex samples from donors stratified by ePRS burden. We found that the ePRS was significantly associated with AD diagnosis and neuropathological measures, comparable to a pathway-agnostic PRS despite representing far fewer loci. High ePRS correlated with increased neuronal endosome volume, number and perinuclear aggregation, as well as enlarged microglial lysosomes, independent of AD pathology. Single-nucleus RNA sequencing revealed cell-type transcriptomic changes associated with ePRS status, including glutamatergic signaling, protein homeostasis, responses to DNA damage and immune function. Neurons, astrocytes, oligodendrocytes, and microglia showed varied gene expression patterns associated with ePRS burden.

Conclusions: This study provides evidence that AD genetic risk variants harboring ELN genes correlate with endolysosomal dysfunction in human brain tissue. These findings suggest that pathway-specific genetic risk contributes to corresponding cellular pathology in AD and nominates candidate mechanisms by which ELN AD variants contribute to pathogenesis.

INTRODUCTION

Recent clinical trials targeting amyloid beta removal in late-onset Alzheimer's disease (LOAD) have shown modest potential benefits, and there is room for more effective interventions. Drug development in LOAD has been hindered by an incomplete understanding of its mechanisms, largely due to the disease's genetic, pathologic and mechanistic heterogeneity. While amyloid beta is present in AD brains and thought to be necessary for the development of the AD phenotype, the progressive degeneration leading to cognitive decline results from multiple cellular responses across several disease phases[1]. Elucidating these aspects of disease progression may reveal additional intervention targets.

Genome-Wide Association Studies (GWAS) and candidate gene approaches have revealed the complex genomic architecture underlying LOAD[1-6] by identifying single nucleotide polymorphisms (SNPs) which tag discrete regions of chromosomes or loci, associated with AD. Genes within these risk loci give pathogenic clues to etiology; genomic regions correlated to AD may harbor genes relevant to AD pathophysiology. Notably, GWAS of LOAD involve hundreds of thousands of individuals but detailed molecular studies of human brain tissue are not currently feasible at that scale due to limitations in tissue availability and resources. Therefore, human genetic variation presents a significant challenge to investigating LOAD pathogenesis when attempting to derive mechanistic insights from patient samples in a reasonably sized cohort. In this study, we developed approaches to this challenge that would leverage, rather than be limited by human variation.

The aggregate burden of common genetic risk identified in GWAS can be estimated using polygenic risk scores (PRS) which calculate a cumulative load of AD genetic SNPs weighted by factors including odds ratio, that predict an association of variant burden with risk for AD incidence [7-9], as well as various AD biomarkers, neuropathology and endophenotypes[10-17]. GWAS have identified variant haplotypes with genes in immune, synaptic function, lipid metabolism, endolysosomal pathways among others[18] nominating those pathways as candidate AD drivers. Whether variant burden in a specific pathway actually correlates to observable pathway changes is largely not known and remains a significant gap in the goal to map the mechanisms linking variant to disease pathogenesis. The endolysosomal network (ELN) plays important cell-type specific roles in brain homeostasis and is already strongly linked to AD pathogenesis[19-21]. However, it is not known if endolysosomal network risk loci contribute to observed ELN pathology

in AD, and if they confer additional gene regulatory or functional changes relevant to AD pathology. Further, the cell type specific consequences of AD variants are not well established yet clearly important to fully understanding pathophysiology. Determining whether or not having a higher burden of ELN risk portends a more likely role for ELN dysfunction could have important implications for future development of targeted therapies.

We hypothesized that a higher burden of ELN risk loci drives endolysosomal pathology in AD and this could be assessed when comparing to AD without high ELN genetic risk burden. In the context of AD pathology we predicted gene expression profiles would be distinct between high and low ELN burden in donors with neuropathologically confirmed AD. To test our hypotheses, we investigated the correlation of an endolysosomal polygenic risk score (ePRS), representing 13 established AD GWAS loci which contain genes of the endolysosomal network, with cell-type specific cellular and molecular phenotypes in neuropathologically confirmed AD and control brain tissue.

Gene	rsID	β	*p*-value
BIN1	rs6733839	0.0650	1.01E-37
BIN1	rs744373	0.0476	1.68E-19
CD2AP	rs10948363	0.0311	3.11E-08
CD33	rs3865444	0.0164	4.49E-03
CLU	rs9331896	0.0245	1.74E-06
EPHA1	rs11771145	-0.0188	2.28E-04
HLA-DRB5	rs9271192	-0.0257	5.31E-06
MEF2C	rs190982	0.0113	3.94E-02
MS4A6A	rs983392	-0.0326	2.37E-09
MS4A4E	rs670139	0.0243	1.28E-06
PICALM	rs10792832	0.0344	1.48E-10
PTK2B	rs28834970	0.0244	3.89E-06
SORL1	rs11218343	-0.0468	8.14E-05

Table 1:

Thirteen variants identified through AD GWAS used to create the ePRS score.

RESULTS

Pathway Specific PRS predicts AD status and AD neuropathologic measures

PRS combine the effects of many SNPs into a single measure of accumulated risk, and their association with AD risk varies by which variants are included and how their signals are combined [22]. PRS limited to AD GWAS hits implicating genes within specific pathways can also

provide useful insight. For example, endocytosis-focused PRS are associated with risk of AD and mild cognitive impairment [17], AD biomarkers [10, 13, 14], and multiple cognitive measures[10]. We hypothesized that the cumulative burden of ELN-affiliated risk alleles impacts cell type-specific ELN function, thus contributing to LOAD pathogenesis. To test this hypothesis, we first developed an ELN pathway-specific polygenic risk score (ePRS) combining information from 13 AD GWAS SNPs (Table 1) and contrasted it with a pathway-agnostic PRS focused on common AD GWAS hits with relatively strong effect sizes (Table 1 + rs7274581, rs10838725, rs6656401, rs8093731, rs17125944, rs35349669, rs2718058, rs10498633, rs1476679)[2, 23, 24]. We calculated both PRS in a local sample of clinically and neuropathologically confirmed AD cases and controls and the AD Sequencing Project data (ADSP; n = 10967 cases, 16432 controls). We tested their association with AD neuropathology after adjusting for sex and *APOE* ε4 carrier status in the UW sample and sex, ε2, ε4, population structure, and relatedness in the ADSP. We found that the significant association between ePRS and multiple AD neuropathology measures in the UW and ADSP samples was comparable to the pathway-agnostic PRS despite representing ~50% of the AD GWAS loci (p-value < 0.05; Figure 1).

ePRS is associated with cell type specific endolysosomal cytopathology

The relationship between abnormal and enlarged early endosome pathology and AD is well established in the literature, both in post-mortem brain and model systems[25-28]. We analyzed early endosomes in neurons from high and low ePRS cases from our tissue cohort (Table 2) using quantitative immunofluorescence and confocal microscopy. Due to the abundance of these organelles in neurons, we analyzed early endosome changes in the somatodendritic and perinuclear neuronal regions separately. Figure 2 A-D shows representative neurons at different ADNC stages (0-3). We observed a higher number of endosomes in neurons with high ePRS (Fig 2E,F), a finding seen in other neurodegenerative disease studies[29], and suggestive of altered function. Increased perinuclear early endosome aggregation with high ePRS was observed across ADNC levels; for example, the representative AD case with low ePRS in Figure 2C has smaller and fewer endosomes in the perinuclear region than the high ePRS individual who also has AD pathology (Figure 2D). This relationship between increasing ePRS and somatodendritic EE density remained significant even when intermediate-high AD cases only were included in the model ("ADNC 2/3 cases", red). Interestingly, the high ePRS genetic background was also significantly correlated with enlarged endosome size in the perinuclear region in cases with intermediate to high AD pathology although not in the somatodendritic region (Fig 2E-F, red bars). Perinuclear aggregation of endolysosomes has been observed in

LOAD hippocampal neurons[30] and we also noted striking aggregation of early endosomes in the perinuclear region of high ePRS cases with AD pathology (Fig 2G).

Microglial lysosomes are larger in high ePRS individuals.

Quantitative analysis of lysosome volume and number per microglia was performed on LAMP1 immunostaining of Iba-1 positive cells in post-mortem human DLPFC tissues (Fig 2H, I) (Table 3). We found that similar to endosome morphology in neurons, microglial lysosome correlated to ePRS. LAMP1 immunoreactivity was used to assess lysosomal content. We analyzed mean lysosomal volume, and the number of lysosomes present per micron of microglial cell while adjusting for age, sex, post-mortem interval and *APOE* genotype. When comparing high versus low ePRS cases regardless of AD pathology, or in just cases with high AD pathology high ePRS was significantly associated with larger lysosomal mean volume but not the number of lysosomes (Fig 2J).

ELN genes in ePRS variant loci are expressed across brain cell types in AD DLPFC tissue.

Single-cell/nucleus omics studies of affected AD brain tissue have dramatically improved our understanding of cellular interactions and responses to pathology[31-34]. They serve as platforms for hypothesis generation, enabling exploration of cell-type specific pathways and gene networks that may be obscured in bulk tissue RNA sequencing. We performed single nucleus sequencing (snRNAseq) from 11 low ePRS, high ADNC and 12 high ePRS, high ADNC DLPFC donors (Table 4). The output of the snRNAseq analysis from the 23 donors demonstrated good representation of all the standard brain cell types (Fig 3A; Emani et al., 2024). We found roughly similar composition of cell types between high and low ePRS donors, though with a statistically significantly smaller cluster of microglia in high ePRS (Fig 3B). We first established the expression profile of the endolysosomal genes associated with the ePRS variants. As expected, there was variable expression across cell types (Fig 3C). *PICALM* and *MEF2C* were expressed in many cell types, most highly in microglia, while other genes were more selectively expressed such as *CD2AP* or *CLU*. The differential pattern of expression underscores that there may be cell-type biased effects of ePRS AD variant burden.

DLPFC brain nuclei demonstrate shared and distinct transcriptomic changes associated with ePRS status

We performed pseudobulk analyses within each cluster (cell-type) to generate DEGs and GSEA and begin to characterize the overall biological pathway differences associated with ePRS score despite the cohort all having similar high AD pathology score. Across all cell types we observed that the high ePRS cohort showed decreased enrichment of Gene Ontology Biological Processes (GOBP) related to “macroautophagy” and “synaptic vesicle lumen acidification”, suggesting that increased ELN variant burden may impact those endolysosomal functions broadly (Fig 4A). Pathways related to protein homeostasis such as "protein refolding" were similarly depressed in high ePRS donors. Evidence of metabolic changes correlating to ePRS was suggested by negative enrichment of electron transport chain pathways and enrichment in glycolysis pathways in select cell types (Fig 4A). These findings identify common alterations in certain endolysosomal, metabolic processes and protein processing pathways across neuron and glial cell types associated with higher ePRS risk allele burden. These changes are likely occurring beyond those that develop as a result of AD pathology as all individuals in this dataset have AD pathology.

Neurons: Several excitatory and inhibitory neuronal subtypes across all layers of cortex were identified. The majority of excitatory neurons (clusters 1,6,8,11) expressed genes associated with layers 4-6 of the cortex[32]. Using pseudobulk analyses we identified genes significantly enriched in high ePRS donors in cluster 1 excitatory neurons including transcription factors or DNA-binding proteins involved in cell differentiation and neuronal fate such as kelch like family member 4 (*KLHL4*), and AT-rich interaction domain family 3B (*ARID3B*)[35, 36]. Genes that regulate neuronal excitability and AMPA receptor trafficking to and from the membrane were altered in cluster 1, including ORAI Calcium Release-Activated Calcium Modulator 2 (*ORAI2*), a component of an inward-rectifying calcium channel[37, 38]. Consistent with these observations, excitatory neurons in cluster 1 and cluster 6 demonstrated enrichment of calcium ion GOBP gene sets in high ePRS individuals (Fig 4A). Additionally, high ePRS excitatory neurons upregulated a distinct set of glutamatergic signaling genes related to synaptic organization such as *SHANK2 and SHANK3*[39, 40] and presynaptic neurotransmitter release, *UNC13A*[41]. Inhibitory neurons were classified as LAMP5 expressing (cluster 3), parvalbumin/somatostatin expressing (cluster 7) or chandelier neurons (cluster 10)[32]. LAMP5 expressing inhibitory neurons showed significant enrichment of the “positive regulation of synaptic transmission glutamatergic” pathway in high ePRS individuals. Genes driving this enrichment included those encoding an NMDA receptor subunit, *GRIN2* and AMPA receptor regulating subunit *CACNG2*[42, 43]. Thus excitatory and inhibitory neuron cell types both appear to respond to high ePRS by modulating glutamatergic signaling gene expression but in a cell-type specific profile. This suggested that

LAMP5 Inhibitory neurons may be increasing gene expression to receive glutamatergic input, while excitatory neurons may be modifying both input and output signaling components. OPCs similarly showed enrichment of the same glutamatergic signaling pathway in high ePRS.

To better understand the distribution of key pathway components across cell populations, we assessed the relative expression of gene modules using the Seurat module score approach and both GOBP and Reactome databases (Fig 4B). The '"Positive Regulation of Synaptic Transmission Glutamatergic" module revealed heterogeneous expression across neural populations, with both neuronal subtypes showing expression as expected, but interestingly, also robust expression in OPCs (cluster 5). It is known that OPCs may synapse with glutamatergic synapses[44], and these data suggest perhaps more so in the context of high ePRS. Further analysis of endolysosomal transport modules revealed cell type-specific expression patterns for GOBP terms, "Endosome to Lysosome Transport" and "Autophagosome-Lysosome Fusion" modules (Fig 4B) were generally lower in neuronal populations compared to glia.

In addition to synaptic and endolysosomal pathways, we found that excitatory and inhibitory neurons in high ePRS individuals showed significant upregulation of DNA damage repair and chromatin remodeling pathways (Fig 4A). Interestingly, visualizing the modules associated with DNA damage, and downstream consequences of DNA damage such as senescence, apoptosis and cell cycle arrest; (GOBP "Intrinsic apoptotic signaling pathway by p53", Reactome, "Cellular Senescence" and " G1 S DNA Damage Checkpoint"), we found higher module scores in glia compared to neuronal populations. Thus while high ePRS showed preferential enrichment of DNA damage pathways, glial cells appear to maintain a baseline higher expression of these modules.

<u>Astrocytes:</u> Astrocytes (cluster 2) GSEA analysis demonstrated that many of the representative pathways in each biological category were significantly altered in astrocytes by ePRS variant burden (Fig 4B). These pathways include "vesicle tethering" and "glutamate receptor signaling", as well as "transport via multivesicular body (MVB) sorting" pathways in the cargo and vesicle trafficking category. Similar to other cell types, pathway analysis also identified pathways involved in DNA repair such as "double strand break repair" and "UV damage excision repair" that are up in high ePRS individuals compared to low ePRS individuals in astrocytes. Multiple immune-related pathways were altered in astrocytes including "response to virus" that was only shared with microglia. Immune pathways are lower in high ePRS individuals than low ePRS individuals. These findings suggest that immune response, metabolism, cargo

transport/degradation, protein homeostasis, and DNA repair processes are all altered in astrocytes by the increased burden of ePRS risk alleles.

Oligodendrocytes and OPCs: Oligodendrocytes (cluster 0) made up the largest population in our dataset. Gene expression in oligodendrocytes was significantly altered by ePRS. Genes more highly expressed in low ePRS included RAS oncogene family members *RAB39A* and *RAB3A* which are both related to vesicle formation and trafficking[45, 46]; *RAB3A* has been implicated in oligodendrocyte maturation and may participate in myelination programs[46]. Like astrocytes, gene sets associated with metabolism differentially enriched in low ePRS included "response to oxidative stress" and "macroautophagy". Oligodendrocytes demonstrated increased enrichment of all representative DNA repair and chromatin organization pathways in high ePRS individuals. "Vesicle tethering" and "lipid response" pathways were enriched in high ePRS while other myelin-related functions including "response to axon injury" and "export across plasma membrane" were lower in high ePRS individuals. Regulation of exocytosis was most strongly enriched in high ePRS oligodendrocytes compared to low ePRS. This is notable as exocytosis is key to myelin formation and expansion[47] and requires regulated transport and release of cargo including proteolipid protein to myelin sheaths[48, 49]. Module scores analysis showed relatively much lower enrichment for this gene set in oligodendrocytes compared to other cell types, supporting the premise that lower baseline expression of a pathway in a particular cell type does not necessarily indicate reduced biological importance or vulnerability to perturbation. Oligodendrocyte progenitor cells (OPCs; cluster 5) shared many pathway signatures with oligodendrocytes, but with some additional shifts associated with ePRS. Notably, OPCs showed significant enrichment for synaptic glutamatergic gene sets similar to inhibitory neurons, suggesting a potential effect of ePRS burden on OPCs responding to neuronal activity. "Amyloid beta clearance" and "endosomal transport" pathways were significantly lower in high ePRS individuals in OPCs. Similar to inhibitory neurons, as discussed above, OPCs showed significant enrichment for synaptic glutamatergic gene sets.

Microglia: Composition analyses had suggested possibly a modest decrease in microglial (cluster 4) proportions in high ePRS. Microglial demonstrated a less marked shift in individual genes as assessed by pseudobulk measures, based on ePRS. Pathways significantly altered demonstrate a profile similar to astrocytes, with increased "UV damage excision repair" and decreased "response to virus" and "amyloid beta clearance" in high ePRS individuals (Fig 4A). High ePRS microglia showed relative decrease of enrichment for "receptor mediated endocytosis", suggesting that higher ELN burden may alter the regulation of internalization in

the context of AD pathology. Microglia also demonstrated a unique signature of “response to prostaglandin” pathway more enriched in high ePRS individuals.

Together, the GSEA and Module score analyses suggest that ePRS burden affects ELN pathways as well as a broader panel of functional pathways regulating neuronal excitability and cellular metabolism across cell types. There may be cell types with lower baseline expression of specific pathways though genetic risk factors can drive significant changes, highlighting the cell type-specific consequences of endolysosomal network genetic burden.

Cell-Cell Communication is distinct between high and low ePRS donors

To begin to understand the intercellular signaling and communication patterns that may be altered by ePRS in AD donors, we applied the CellChat (V2) computational tool to infer cell-cell communication networks[50]. The CellChat V2 version includes existing databases such as CellPhoneDB and NeuronChatDB[51]. The methods identify the “senders” and “receivers” of signaling and incorporate other data of known mediators of that signaling network. We compared signaling patterns between high and low ePRS individuals, all of whom had high AD pathology, again to enable identification of differences more likely to be related to ELN variant burden.

High ePRS was associated with differentially higher number of interactions primarily from Layer 5/6 and Layer 5/6 Near Projection neurons both in communicating to other excitatory neurons as well as inhibitory neuronal populations (Fig 5A). In contrast, high ePRS oligodendrocytes demonstrated decreased interactions with other glial cells, particularly OPCs. We examined specific pathways and found variable effects of ePRS on cell-cell communication. For example, NRXN signaling, an important component of synaptic signaling was enriched in high ePRS, consistent with pseudobulk and correlation gene expression analyses (Fig 4). In contrast, VEGF signaling between astrocytes and the cluster identified as blood vessel cells, was more prominent in low ePRS individuals (Fig 5C).

ePRS correlates to changes in gene expression changes in ADNC donors across cell types

Pseudobulk DEG analysis, a relatively conservative method that corrects for Type 1 error, demonstrated significant differences in degrees of gene and pathway expression across cell types based on ePRS status. While our initial analyses used a binary approach comparing high versus low ePRS quartiles, we also investigated how the continuous ePRS measure correlates with gene expression. We calculated Pearson’s correlation coefficient between donor ePRS and

gene expression CPM (counts per million). Despite the discontinuous ePRS distribution we observed robust transcriptomic associations with ePRS score in multiple cell types.
Figure 6A shows gene expression heat maps from four different cell types. Donors (columns in heatmap) are arranged by increasing ePRS score left to right (Fig 6A). Patterns of coordinated gene expression appear to correlate with ePRS burden in all cell types (shown is oligodendrocyte, astrocyte and neuronal clusters, microglia and others are in Supplementary). Statistical analysis identified significant correlations ($r > 0.6$, $p < 0.01$) between ePRS and expression of key genes in multiple functional categories (Fig 6B). These included endolysosomal genes such as *RAB7A* and *VPS35* which are positively correlated to ePRS and both critical regulators of endosomal trafficking. In contrast, we found negative correlation of expression of *COPA,* a gene involved in retrograde vesicular trafficking[52] (Fig 6B). Genes involved in protein homeostasis demonstrated correlation to ePRS in multiple cell types such as co-chaperone *DNAJC12*[53], proteosome component *FXBO7*[54] and *ITMB2B*, a gene whose product interacts with APP and is involved in mitochondrial homeostasis[55]. Chromatin remodeling and cell cycle genes such as transcription factor *CTCF* in LAMP5 neurons and *CCND1* in OPCs also showed positive correlation with ePRS consistent with our GSEA findings of altered DNA damage pathways (Fig 6B). In addition we found positive correlation of genes involved in glutamatergic signaling such as *KCNB1* (r: 0.71, p value 0.00013) and *SHANK2* (r: 0.67, p value 0.00054) in Layer 5/6 (Supplemental data). Expression patterns and direction of association were similar to the biological pathways we found in the GSEA from binary comparison further supporting the notion that ePRS may interact with responses to DNA damage, chromatin remodeling and immune pathways.

DISCUSSION

Here we report the first study in human donor brain tissue, to our knowledge, that assesses the cell type specific molecular and cytopathological features associated with a pathway specific AD polygenic risk score that is also sensitive to predicting AD diagnosis and pathology. We show that a PRS representing endolysosomal pathway AD risk variants is associated with endolysosomal changes across cell types in pathologically confirmed AD. A strength of our approach is the application of complementary analyses with different statistical limitations. We employed pseudobulk for differential expression, a comparatively more conservative method that minimizes false positives as well as single-cell methods such as gene to ePRS correlation and cell-cell communication inference. These analyses revealed similar themes and

associations giving confidence to our findings despite the limitations to smaller sample number and the inherent heterogeneity of human brain samples.

The ELN is an established candidate mechanistic driver of AD and other neurodegenerative diseases[20]. The discovery of AD risk variants harboring ELN genes gave human genetics support to the premise as well as potential leads to the molecular pathways linking genetic risk to neural cell dysfunction. The ELN is a fundamental component of cellular homeostasis and some cell types have developed specialized functions dependent on the ELN such as synaptic receptor recycling, exocytosis, lysosomal degradation in phagocytes[20, 21, 56-59]. Therefore the first step in leveraging genomic variation to reveal AD mechanisms is to better understand the cell-type specific changes in ELN related genes and pathways with cell-type specific resolution. Establishing these associations is critical to mapping how the molecular effects of AD variants contribute to AD pathogenesis.

ELN cytopathology as an early feature of AD has been well established for years[25]. However, to what degree abnormal endosome and lysosome morphology is simply a secondary consequence of proteopathy progression rather than contributor to the disease process is not fully understood. Despite this, studies in tissue show endosomal pathology in MCI and Down's syndrome subjects prior to the development of amyloid plaques and hiPSC models of AD-related endosome dysfunction similarly show enlarged endosomes in cells that do not yet have much amyloid pathology[25, 28, 60] The discovery of common AD risk alleles harboring ELN genes and AD rare variants in ELN genes (*SORL1, ABCA7*) provides strong human genetic evidence supporting a pathogenic role for intrinsic changes to ELN function. Here we show that common genetic risk in ELN loci have significant correlations with endolysosomal morphology and gene expression in pathways dependent on ELN function, such as autophagy, synaptic function and immune response. Importantly, these changes vary within the diverse cell types of the central nervous system, highlighting both the importance of this pathway for brain homeostasis and the complexity of developing it as a therapeutic target. Our findings of increased numbers, aggregation and enlargement of early endosomes in neurons suggests deficiencies in function of these important organelles. Indeed, other work by our group and others show altered neuronal endosomal function in models lacking key endosomal genes[61, 62]. Importantly, some of the endosomal pathologies we observe are present in low ADNC subjects, further suggesting that they are driven by genetics rather than amyloid pathology.

Interestingly, we find strong transcriptomic signatures showing altered glutamatergic signaling in high vs. low ePRS neuronal populations. This corroborates work in model systems showing that depletion of endosomal trafficking complexes, such as retromer, or endosomal genes, such as *SORL1,* leads to altered localization of AMPARs and deficits in long-term potentiation, the cellular basis of memory[62-64]. Additionally upregulation of glutamatergic signaling in excitatory and inhibitory neurons could suggest that altered endolysosomal function may lead to compensatory changes in synaptic transmission machinery.

The enlarged endosomes in neurons and lysosomes in microglia align with expression changes in trafficking genes like *VPS35* and *RAB7A,* suggesting that genetic risk directly impacts both the physical organization and molecular machinery of the endolysosomal system of multiple cell types. While microglia demonstrated enlarged lysosomes in high ePRS individuals though showed fewer differential genes between high and low ePRS. It is possible that microglia are particularly susceptible to modest changes caused by ePRS loci. Enlarged lysosomes may reflect impaired acidification, degradation[65], pathways differentially impacted by ePRS as measured by gene expression. There was a modest reduction in microglia numbers in the high ePRS cohort, which if not driven by technical issues, could suggest changes in microglial survival, proliferation or recruitment. Both astrocytes and microglia showed enrichment in apoptotic pathways which could explain cell number differences though this will need to be validated though intact tissue studies such as immunohistochemistry. The enrichment of apoptotic and senescence pathways in conjunction with DNA damage responses suggests that ePRS may influence responses to accumulating DNA damage. Whether this would also be the case in normal aging is an important question and relates to earlier work suggesting endolysosomal and immune risk variant burden is associated with cognitive health in aging in a unique population of centenarians[11]. Notably, our method did not enrich for microglia and therefore the numbers of microglia per person averaged ~350 nuclei, typical for nuclei approaches that do not enrich for or against cell types, which limits resolution of microglial states. Thus, the “microglia” cluster itself is likely heterogeneous and within it different microglial states which may reduce sensitivity to ePRS driven changes. It is possible that ePRS may impact specific microglial states or proportion of states which may be revealed with enrichment or spatial techniques[66].

Module score analysis enabled better understanding of GSEA and gene expression patterns. We could appreciate that some pathways may be expressed across multiple cell types though

differentially impacted by ePRS status in a cell-type specific manner. Though many pathways are expressed across multiple cell types, the effect of ePRS was more prominent in some cell types more than others, or conversely that ePRS was associated with broad effects on a pathway that had variable enrichment across cell types. For instance the glutamatergic signaling module was active in excitatory and inhibitory neurons and OPCs, though GSEA showed significant enrichment of this pathway in inhibitory neurons suggesting differential vulnerability to ELN pathway changes. In contrast, macroautophagy showed consistent negative enrichment in high ePRS cell types suggesting a possible fundamental consequence of ELN dysfunction. Module score analysis meanwhile revealed higher baseline expression of the macroautophagy gene set in microglia (Supplemental Data) which may reflect their specialized roles in clearance.

CellChat analyses highlighted differences in strength and number of connections between neural cells. While both CellChat and GSEA are based solely on gene expression, CellChat also takes into account downstream targets of the signaling pathway and renders further hypotheses generating analyses[50]. PV/SST neurons showed increased strength of signaling though fewer number of interactions in high ePRS (Fig 5). We had noted in the pseudobulk analysis that genes driving the enrichment of glutamatergic signaling in these inhibitory neurons included postsynaptic elements, *GRIN2A/B*, which could again suggest compensatory increases in receiving glutamatergic signaling as a compensatory mechanism. We observed increased neuronal-oligodendrocyte and OPC communication. This cross talk between neurons and oligodendrocyte/OPC could reflect compensatory attempts at remyelination, modulation of neuronal activity or other interactions which contribute to vulnerability or resilience. For instance, neuronal signaling can induce exocytosis of myelin membrane[49] from oligodendrocytes while OPCs can induce exocytosis of neuronal lysosomes and related metabolism[67].

Endolysosomal dysfunction has been associated with various forms of programmed cell death[68]. The co-occurrence of altered DNA damage and chromatin remodeling pathways with endolysosomal dysfunction across multiple cell types in high ePRS individuals suggests a potential connection between AD ELN variants and cellular stress responses that warrants further investigation. Notably protein homeostasis pathways such as protein folding, chaperone mediated processes were uniformly depressed in the high ePRS (or enriched in the low ePRS)

which could indicate that impaired ELN function and related disruption of protein handling could also contribute to cell stress.

There are limitations to this study. New loci have emerged in recent AD GWAS, while fine-mapping and colocalization experiments have implicated additional genes at established loci[69]. Genes influence the ELN (ex., *TREM2*[70]) and should be considered as additions to our ePRS and will be in future iterations of PRS. Several loci have multiple independent signals that may not be adequately captured by the SNPs in our ePRS. For example, while *CLU* rs9331896 and *PTK2B* rs28834970 are often considered the same locus, the two SNPs are not in LD in 1000 Genomes European samples[71, 72]. Confident linking of ELN genes to the tagging SNPs used in GWAS will require additional epigenetic analyses with emerging single cell chromatin accessibility, methylation and 3D chromatin conformation methods.
This study is focused on donors with only high AD pathology and therefore reflects end-stage disease. Ideally, a larger cohort across the spectrum of pathology can provide even greater insight into the earlier and later changes that correlate to ELN burden. We attempted to control for secondary effects of AD neurodegenerative processes on the ELN in our assessment of ePRS by conducting high ADNC only comparisons across ePRS. Whether by neuropathology or gene expression, we find that despite the same neuropathological burden and diagnosis, higher ePRS appears to drive endolysosomal changes in neurons and microglia.

Conclusions

Our work demonstrates that an AD endolysosomal variant pathway-specific genetic risk score does correlate to cytopathologic and molecular changes that are associated with endolysosomal function in those with higher ELN variant risk (high ePRS). While genes in the ELN that are within AD risk loci have supported the ELN role in AD pathogenesis (in addition to findings in vitro and in animal studies), direct assaying of ELN function proxies such as morphology and cell gene expression in relation to ELN variant risk had not yet been established. This information is valuable to dissecting the molecular consequences of these non-coding variants and the mechanisms by which they contribute to AD, including how they may lead to local or distal gene regulation, either directly or indirectly. The effects of high ePRS resulted in shared and distinct molecular patterns in different cell types. It will be essential to leverage human neural cell models and determine whether this relationship is observed in neurons, glia and other cell types carrying varying burdens of ELN variants, where external factors such as the

lived experience are removed. Once a biomarker confirmed diagnosis is made, the ePRS could be used to stratify clinical trials participants into endolysosome targeting therapies. It is likely that various ELN components will have differential import to different cell types and identifying which are most targetable, occur earliest, and most applicable across patients will be similarly important to translating the rapidly gathering evidence implicating the ELN in AD into clinically actionable findings.

METHODS

Tissues

Brain tissue was collected from human donors post-mortem after appropriate consent was obtained during life. All tissues were obtained for processing from the Precision Neuropathology Core at the University of Washington. Cases with diagnoses of non-AD tauopathies, FTLD and ALS were excluded, as well as cases with known genetic chromosomal abnormalities. Additionally, comorbid pathology cortical stroke, history of malignancy, cerebral infection, were exclusionary (Demographic data for each analysis is provided in Tables 2-4 and de-identified individual level data in Supplemental data). All cases had cognitive data available, as well as rigorous neuropathology work-ups in accordance with consensus guidelines including AD Neuropathologic Change (ADNC) scoring. ADNC reflects severity of hallmark AD amyloid-beta plaques and phosphor-tau neurofibrillary tangles, assessed histologically. An ADNC Not ("0") score indicates no evidence of AD pathology. At the ADNC Low ("1") stage AD pathology is present but not sufficient for AD diagnosis. ADNC 2 and 3 scores are more tightly correlated with dementia and clinical presentation of AD in clinico-pathologic correlation studies. In accordance with common practice in LOAD neuropathologic studies we designate ADNC 2-3 cases " AD" group ADNC 0-1 cases as "controls"[73-76].

Genotyping

Four mm punches from fresh frozen cerebellum or dorsolateral prefrontal cortex (DLPFC) were lysed and genomic DNA (gDNA) extracted using the GeneJET gDNA Purification Kit (Thermo Scientific #K0722). One microgram of gDNA was sequenced using the Infinium Global Diversity Array 8 v1.0 to detect common single-nucleotide polymorphisms (SNP) and sequenced at the Northwest Genomics Center, Seattle, WA.

Development and calculation of the ePRS

Endolysosomal pathway-specific polygenic risk score (ePRS[77]) was developed combining information from 13 AD GWAS SNPs correlated to ELN genes (**Table 1**) using the explained-variance approach[2, 8].

Immunohistochemistry

Immunostaining and IMARIS analysis of endosome and lysosomes. Immunohistochemistry was performed for endosome and lysosome morphology in fresh frozen DLPFC (neuronal endosomes) or paraffin embedded DLPFC (microglia lysosomes) based upon the optimal tissue type for the endolysosomal antibody.

1. *Neuronal endosome morphology analysis from postmortem brain tissue:*

Postmortem brain tissue from 14 low ePRS and 13 high ePRS donors with PMI <8 hours and available fresh frozen inferior parietal lobule tissue were immunolabeled for endosome morphology (Table 2). The immunohistochemistry, imaging and image analysis methods used for quantifying early endosome morphology in postmortem brain tissue are described in detail in previously published work[78]. Major steps are described in brief here.

Fresh frozen inferior parietal lobule samples were cut at 5 um thickness and fixed with 4% PFA. Tissue was blocked in 5% normal goat serum (NGS, Jackson ImmunoResearch Laboratories # 005-000-121) + 2.5% bovine serum albumin (BSA, Sigma-Aldrich # A3294) + 0.1% Triton X-100 (Fisher Bioreagents # BP151-100). Primary antibodies used were mouse anti-EEA1(BD Biosciences # 610456) and chicken anti-MAP2 (Abcam # ab92434) diluted 1:500. Secondary antibodies used were goat anti-Chicken IgY (H+L) secondary antibody Alexa Fluor™ 594 (Invitrogen # A11042) and goat anti-Mouse IgG (H+L) Secondary Antibody Alexa Fluor™ 488 (Invitrogen # A11029) diluted 1:1000. Autofluorescence was quenched with TrueBlack (Biotium # 23007) 1:20 according to manufacturer guidelines.

Neuron IHC cohort		Low ePRS (n = 14)	High ePRS (n = 13)
ePRS	Mean +/- SD	8.0 +/- 1.5	15.7 +/- 1.6
Age at death	Mean +/- SD (yrs.)	90.0 +/- 8.1	83.2 +/- 12.4
PMI	Mean +/- SD (hrs.)	4.4 +/- 1.2	6.0 +/- 1.0
Sex	Female % (#)	71% (10)	62% (8)
	Male % (#)	29% (4)	38% (5)
Cognitive status	Norm cognition % (#)	50% (7)	62% (8)
	Dementia % (#)	50% (7)	38% (5)
APOE	E2/E3 % (#)	7% (1)	0% (0)
	E3/E3 % (#)	71% (10)	77% (10)
	E3/E4 % (#)	21% (3)	23% (3)
	E4/E4 % (#)	0% (0)	0% (0)
ADNC	0 % (#)	21% (3)	8% (1)
	1% (#)	17% (1)	23% (3)
	2 % (#)	36% (5)	38% (5)
	3 % (#)	36% (5)	31% (4)

Table 2. Demographics of cohort immunolabeled for neuronal endosomes.

Confocal imaging - Neuron

MAP2-positive pyramidal neurons within the cortical gray matter were imaged on the Leica TCS SP8 confocal microscope with a 63x/1.40 oil lens. Z-stack images were captured in the Leica Application Suite X (LAS X 3.5.5.19976) at 5x zoom with LIGHTNING adaptive deconvolution post-processing, using image acquisition settings as described in previous publication[78]. Total z-size was 1.68 µm with 14 steps and a z-step size of 0.13 µm. An average of ten neurons were imaged per case (range 8-13, due to variability in the size of cortex sampled and proportion of gray matter present).

Image analysis and endosome quantification – Neuron

Endosomal morphology was analyzed from confocal Z-stacks using Bitplane Imaris software (Oxford Instruments). EEA1-positive endosome puncta were identified and segmented in Imaris to quantify the total puncta counts and individual puncta volumes. This quantification was performed within two neuronal regions of interest (ROIs): the MAP2-positive somatodendritic ROI and the perinuclear ROI. The perinuclear ROI boundaries were achieved by expanding a surface from the DAPI-positive nucleus to capture the subpopulation of early endosomes localized most closely with the nucleus.

In order to investigate changes in the early endosome size specifically within the largest subset of early endosomes, we defined an “Enlarged early endosome” subpopulation using the traditional definition of a statistical outlier: early endosomes were considered “Enlarged EEs” if their volume was above 2 standard deviations from the mean volume calculated using ADNC 0-1/low ePRS cases (cases most likely to reflect an early endosome size distribution found in healthy aged controls).

A univariate linear regression model was used to assess relationship between ePRS and early endosome morphology output variables (Mean EE volume, Mean EE # per unit ROI volume, Mean “Enlarged EE” volume, and proportion of “Enlarged EEs” compared to total EE #), and adjusted for confounding factors age, sex, PMI, and *APOE* genotype. Statistical analyses were performed on the full cohort (n = 27; ADNC low-high cases) as well as an “AD-only” subcohort (n = 19, ADNC intermediate-high cases). The Mann-Whitney test was used for comparison of early endosome morphologies in low versus high ePRS cases and in non-AD versus AD cases.

Microglia IHC cohort		**Low ePRS** (n = 13)	**High ePRS** (n = 13)
ePRS	Mean +/- SD	8.2 +/- 1.6	15.8 +/- 1.6
Age at death	Mean +/- SD (yrs.)	92.5 +/- 5.8	81.5 +/- 11.2
PMI	Mean +/- SD (hrs.)	4.4 +/- 1.3	5.9 +/- 1.6
Sex	Female % (#)	62% (8)	54% (7)
	Male % (#)	38% (5)	46% (6)
Cognitive status	Norm cognition % (#)	62% (8)	54% (7)
	Dementia % (#)	38% (5)	46% (6)
APOE	E2/E3 % (#)	8% (1)	8% (1)
	E3/E3 % (#)	69% (9)	62% (8)
	E3/E4 % (#)	23% (3)	31% (4)
	E4/E4 % (#)	0% (0)	0% (0)
ADNC	0 % (#)	15% (2)	23% (3)
	1 % (#)	8% (1)	8% (1)
	2% (#)	31% (4)	15% (2)
	3 % (#)	38% (5)	38% (5)

Table 3. Demographics of cohort immunolabeled for microglial lysosomes.

2. *Microglial lysosome morphology analysis from post-mortem human brain tissue:*

Immunohistochemistry of microglia and lysosomal markers was performed on formalin-fixed paraffin embedded tissue from the dorsolateral prefrontal cortex of 13 low ePRS and 13 high ePRS donors (Table 3) following previously published protocols[66] with the addition of the LAMP1 antibody to Iba-1 and DAPI (Lamp-1: Thermo 14-1079-80, 1:250). An Alexa-fluor Donkey anti-Mouse 555 antibody was used for the LAMP1 (ThermoFisher A31570, 1:500).

Confocal Imaging - Microglia

Slides were imaged using a 40x oil lens on the Leica SP8 laser confocal microscope to create Z-stacks with a step size of 0.47µm, 2.2x zoom, 600 Hz speed, and 1024x1024 format.

Image analysis and lysosome quantification - Microglia

The IMARIS software version 10.1 was used to generate surfaces for Iba-1 using a standardized machine-learning segmentation parameter. The machine-learning parameter was created by selecting the background and foreground across z-stacks. Areas without Iba-1 signal or with noise were selected as background, while areas with Iba-1 signal were selected as foreground. Using the "train and predict" feature, we generated a 3D surface of the Iba-1 signal. Microglia were analyzed if DAPI was fully enclosed in the Iba-1 surface and the whole microglia was present inside the image (no processes cut off by the image edge). When the Iba-1 surface was identified to be less than 7 microns distant from a process, the two surfaces were united. Other background Iba-1 signals were eliminated. The LAMP1 signal contained within the microglial surfaces was identified and surfaces were created for the LAMP1 signal using a similar machine learning approach. For LAMP1, surfaces under 1µm^3 in volume were confirmed to be largely single fluorescent puncta, whereas surfaces larger than 1µm^3 in volume were assessed to be largely dual or clusters of fluorescent puncta. Lysosomes were therefore analyzed in two groups: volumes under 1µm^3, and clusters with volumes between 1 and 15µm^3.

A univariate linear regression model was used to assess relationship between ePRS and lysosome morphology output variables (Mean lysosome volume, Mean lysosome # per unit ROI volume), and adjusted for confounding factors age, sex, PMI, and *APOE* genotype.

<u>Single-nucleus transcriptomic studies</u>

Nuclei isolation and enrichment

For single-nucleus RNA-seq (snRNA-seq), methods largely followed those of Prater, Green et al. (2023). Fresh frozen human DLPFC samples from 11 low ePRS and 12 high ePRS (Table 2)

were isolated as previously described[66]. Briefly, four 2-mm punches of DLPFC gray matter were collected using a biopsy punch (Thermo Fisher Scientific) into a 1.5-ml microcentrifuge tube on dry ice. The nuclei in nuclei suspension solution was layered onto 900 µl of percoll/myelin gradient buffer[79]. The gradient was centrifuged at 950*g* for 20 min at 4 °C without break and with slow acceleration. The supernatant with myelin was aspirated, and the nuclei pellet was resuspended in resuspension buffer at a concentration of 1,000 nuclei per microliter and proceeded immediately to snRNA-seq. All samples were processed using the 10X Genomics Chromium Next GEM Single Cell 3' Kit v3.1 (#1000268) with a target capture of 10,000 nuclei. Samples were sequenced using either the Illumina NovaSeq 6000 or NovaSeq X platform through the Northwest Genomics Center.

snRNAseq cohort		**Low ePRS** (n = 11)	**High ePRS** (n = 12)
ePRS	Mean +/- SD	8.5 +/- 0.7	16.2 +/- 1.8
Age at death	Mean +/- SD (yrs.)	89.5 +/- 8.0	84.8 +/- 12.5
PMI	Mean +/- SD (hrs.)	4.7 +/- 1.4	6.1 +/- 1.7
Sex	Female % (#)	64% (7)	58% (7)
	Male % (#)	36% (4)	42% (5)
Cognitive status	Norml cognition % (#)	45% (5)	42% (5)
	Dementia % (#)	55% (6)	58% (7)
APOE	E3/E3 % (#)	64% (7)	58% (7)
	E3/E4 % (#)	36% (4)	33% (4)
	E4/E4 % (#)	0% (0)	8% (1)
ADNC	2 % (#)	36% (4)	42% (5)
	3 % (#)	64% (7)	58% (7)

Table 4. Demographics of snRNAseq cohort.

Alignment, quality control. Methods largely followed those previously published[66]. CellRanger 7.0.2 was used to align the samples using the 2020-A genome provided by 10X Genomics. Analysis was performed in R (R Development Core Team, 2010). Droplets from the samples were combined using Seurat version 4.0.0. The dataset was thresholded to remove droplets containing fewer than 350 genes and droplets with more than 1% mitochondrial reads. Ambient RNA and doublets were detected as previously described[66]. After QC, the total number

of nuclei was 149,533 with 2579.71 average genes/nucleus. A clustering resolution of 0.1 was used after reducing the dimensions of the dataset to 34 principal components.

Normalization, Clustering, and Differential Gene Expression testing with GSEA.
Analysis proceeded as previously described with noted exceptions[66]: Seurat v4.0.0 was used for all analyses. Harmony was used for batch correction in these datasets. For cell type identification in unsorted datasets and prior to subsetting microglia from other cell types after enrichment, marker gene expression from BICCN were used to detect cell types in clusters[32]. All datasets were clustered using the Louvain algorithm with multilevel refinement. GSEA using ClusterProfiler used the 2024 versions of the pathway datasets for GO-BP, Reactome, and Wikipathways. To assess differences in cell-type composition between ePRS groups, we calculated the percentage of cells from each condition (high vs. low ePRS) within each annotated cell type. Cell-type proportions were computed and results were visualized using stacked bar plots. Statistical differences in cellular composition were assessed using a chi-square test.

Single cell analyses:
Violin plots visualization of gene expression: (Fig 3A) Gene expression distributions were visualized using violin plots generated with the VlnPlot_scCustom() function from the scCustomize package in R.

Cell-Cell communication Inference
Cell–cell communication analysis was conducted using CellChat V2 to compare signaling interactions between high ePRS and low ePRS donors across all cell types[50]. CellChat V2 was run separately on each donor group to infer ligand–receptor interactions and compute communication probability scores. The results from both groups were then integrated for comparative analysis. The analysis followed the approach outlined in the CellChat tutorial using all the default parameters.
To identify differentially active signaling pathways between High ePRS and Low ePRS donors, we used the rankNet function in CellChat with default parameters. A Wilcoxon rank-sum test was performed to assess statistical significance, and pathways with an adjusted p-value < 0.05 were considered differentially enriched. For network visualization, we applied a communication probability threshold of 0.05 to focus on high-confidence interactions.This analysis followed the approach outlined in the CellChat comparison tutorial.

Module Scoring

To assess pathway activity, we computed module scores using the AddModuleScore function from Seurat (v5.0.2)[80] with default parameters (nbin=25, ctrl=100). Gene sets were obtained from the Molecular Signatures Database (MSigDB v7.4), focusing on the GO Biological process, Reactome collections.

Correlation of ePRS to cell-type specific gene expression

To identify genes with expression levels correlated with ePRS in each cell type, we calculated Pearson correlation coefficients between pseudo-bulk counts per million (CPM) and donor ePRS. Due to variability in cell numbers captured per donor, we applied filtering criteria to donors and genes before correlation analysis. Only genes that were expressed with at least one count in at least one donor were included. Pearson correlation coefficients were computed between gene expression levels and donor ePRS for each cell type. Genes with a correlation coefficient greater than 0.6 and an unadjusted p-value < 0.01 were considered significant.

FIGURE LEGENDS

Figure 1: Association between ePRS, PRS, and AD neuropathology. X-axis: effect size (point) and 95% confidence interval (line) for association with ADNC [73], Braak [81], CERAD [81], and Thal [82] scores. Covariates include sex + ε4 carrier status (UW) or sex, ε2 and ε4 dose, population structure, and relatedness (ADSP).

Figure 2: ePRS shifts the size and number of early endosomes in the perinuclear compartment in post-mortem cortical neurons and the size of lysosomes in post-mortem cortical microglia. A-D) Representative pyramidal neurons from postmortem parietal cortex. MAP2 (magenta) labels somatodendritic region of the neuron compartment, EEA1 (green) labels early endosomes (EEs), and DAPI (blue) labels nuclei. Perinuclear region of interest (ROI) noted with asterisk; somatodendritic ROI noted with arrow. A, C) Neurons from low ePRS cases have minimal EE aggregation in the perinuclear region, shown in both A) no-low AD (ADNC 0/1) and C) AD (ADNC 2/3) cases. B, D) Neurons in high ePRS cases have distinct

increase in perinuclear EE aggregation (white arrowheads), shown in both B) no-low AD (ADNC 0/1) and D) AD (ADNC 2/3) cases. E-F) Correlation between ePRS and EE morphology metrics using a linear regression model. E) High ePRS correlates with a significant increase in somatodendritic EE number in the full cohort ("All cases", black). F) High ePRS correlates with a significant increase in perinuclear EE number and size in the full cohort ("All cases", black). G) The percentage of neurons imaged per case with clear perinuclear EE aggregation (neurons assigned yes/no for presence of aggregation) was significantly increased in the high ePRS cases compared to low ePRS. ADNC 2/3 cases in red to show that AD cases are represented in both low and high ePRS groups. H) Representative image of a microglia in an individual with low ePRS and AD pathology. I) Representative image of a microglia with high ePRS and AD pathology. J) High ePRS is correlated with increased mean lysosomal volume in both all cases and individuals with AD pathology. Scale bars are 3 μm in all images. *$p<0.05$, **$p<0.01$, ***$p<0.001$, ****$p<0.0001$.

Figure 3. Cell-type composition and endolysosomal gene expression patterns across brain cell populations. A) UMAP of the 149,533 nuclei from 23 high ADNC donors (11 low ePRS and 12 high ePRS). B) Cell composition comparison between high (gold) and low (purple) ePRS donors (Parvalbumin/SST neurons "PV/SST"; blood vessel cells "BV"; Excitatory Neurons "Exc Neuron"; Lamp5 inhibitory neuron "Lamp5"; Chandelier inhibitory neuron "Chandelier"). Microglia proportion is significantly decreased in high ePRS ($p<0.05$). C) Expression patterns of endolysosomal genes within ePRS loci across cell types. *MEF2C* and *PICALM* are broadly expressed across multiple cell types, while *CLU* shows highest expression in astrocytes, and *SORL1* is predominantly expressed in neurons and oligodendrocytes. The width of each violin plot indicates relative frequency of expression levels, with color denoting cell type as shown in panel A.

Figure 4: High ADNC cases demonstrate shifts in gene expression associated with ePRS risk burden. A) Pathway analysis of genes shifting expression together in high ePRS individuals versus low ePRS individuals across the different cell types (columns) reveals categories of gene set enrichment sets that were significantly different between high and low ePRS. Positive enrichment in high ePRS is indicated in yellow, negative enrichment in green. Some pathways, such as protein refolding and macroautophagy, are differentially depressed

across cell types in high ePRS while others such as vesicle, lipid, and DNA-related pathways are significantly enriched in high ePRS in glial populations. Pathways demarcated with a colored square are trending at the $q<0.1$ level while a * indicates that a pathway was significant at $q<0.05$. (OPC oligodendrocyte progenitor cell; Exc. excitatory; Inh. inhibitory). Cluster 2: astrocytes, Cluster 0: oligodendrocytes, Cluster 5: OPC, Cluster 4: microglia. Module score visualizations showing expression distribution of B) ELN gene sets and DNA damage, senescence, apoptotic pathways across cell populations in different cell types. Module scores are represented as a gradient from blue (low expression) to red (high expression).

Figure 5: ***ELN variant burden influences interactions between brain cell types in high ADNC donors.*** A) Heatmap of interactons between cell types. Rows indicate "senders" of signal, columns are "receivers". Red indicates increased interaction number in high ePRS while blue indicates decreased interaction number. Color intensity represents the magnitude of difference. Excitatory neuron populations show increased self and cross-population communication in high ePRS (red), while PV/SST inhibitory neurons exhibit reduced interaction diversity (blue). Both OPCs and oligodendrocytes maintain communicaton with excitatory neurons though interact less with each other in high ePRS. B) Relative contribution of major signaling pathways in high versus low ePRS conditions. Pathways are ordered by the degree of difference between conditions, with gold representing high ePRS and purple representing low ePRS. C-D) Network visualization of representative pathways in low versus high ePRS conditions. Edge thickness and color intensity represent interaction strength between cell types. C) NRXN (left) shows enhanced connectivity among excitatory neurons in high ePRS, while VEGF (right) shows enhanced connectivity between astrocytes and blood vessel cells (BV). Some cell-cell communication networks were unique to or significantly biased towards high or low ePRS. D) VISTA signaling is detected only in high ePRS (left). In contrast, SEMA5 (Semaphorin) and Fractalkine signaling networks are primarily active in low ePRS, with SEMA5 showing strong OPC-neuron interactions and Fractalkine microglia-neuron communication patterns that absent in high ePRS.

Figure 6: ePRS correlates to gene expression in neural cell types. A) Heat map displaying gene expression (rows) for each individual (columns) ordered by ePRS demonstrating progressive transcriptomic change with increasing ePRS. Four cell types are shown as

examples. B) Correlation plots showing significant relationships between ePRS scores (x-axis) and gene expression (y-axis, counts per million) for representative genes in three biological pathways: endolysosomal function, protein homeostasis, and chromatin/DNA regulation. Each point represents an individual donor, with regression lines and 95% confidence intervals shown. Pearson correlation coefficients (r) and p-values are indicated for each relationship.

Figure 1

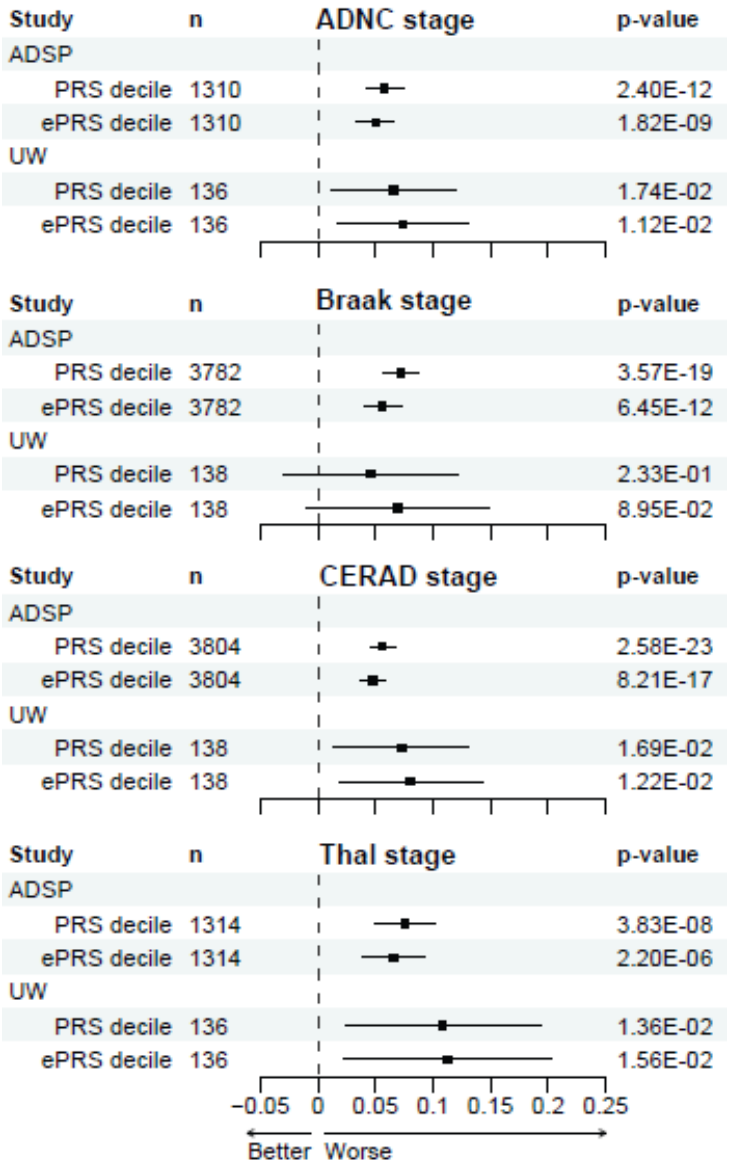
Study
n
ADNC stage
p-value
ADSP
PRS decile 1310 2.40E-12
ePRS decile 1310 1.82E-09
UW
PRS decile 136 1.74E-02
ePRS decile 136 1.12E-02
Study
n
Braak stage
p-value
ADSP
PRS decile 3782 3.57E-19
ePRS decile 3782 6.45E-12
UW
PRS decile 138 2.33E-01
ePRS decile 138 8.95E-02
Study
n
CERAD stage
p-value
ADSP
PRS decile 3804 2.58E-23
ePRS decile 3804 8.21E-17
UW
PRS decile 138 1.69E-02
ePRS decile 138 1.22E-02
Study
n
Thal stage
p-value
ADSP
PRS decile 1314 3.83E-08
ePRS decile 1314 2.20E-06
UW
PRS decile 136 1.36E-02
ePRS decile 136 1.56E-02
−0.05 0 0.05 0.1 0.15 0.2 0.25
Better
Worse

Figure 2

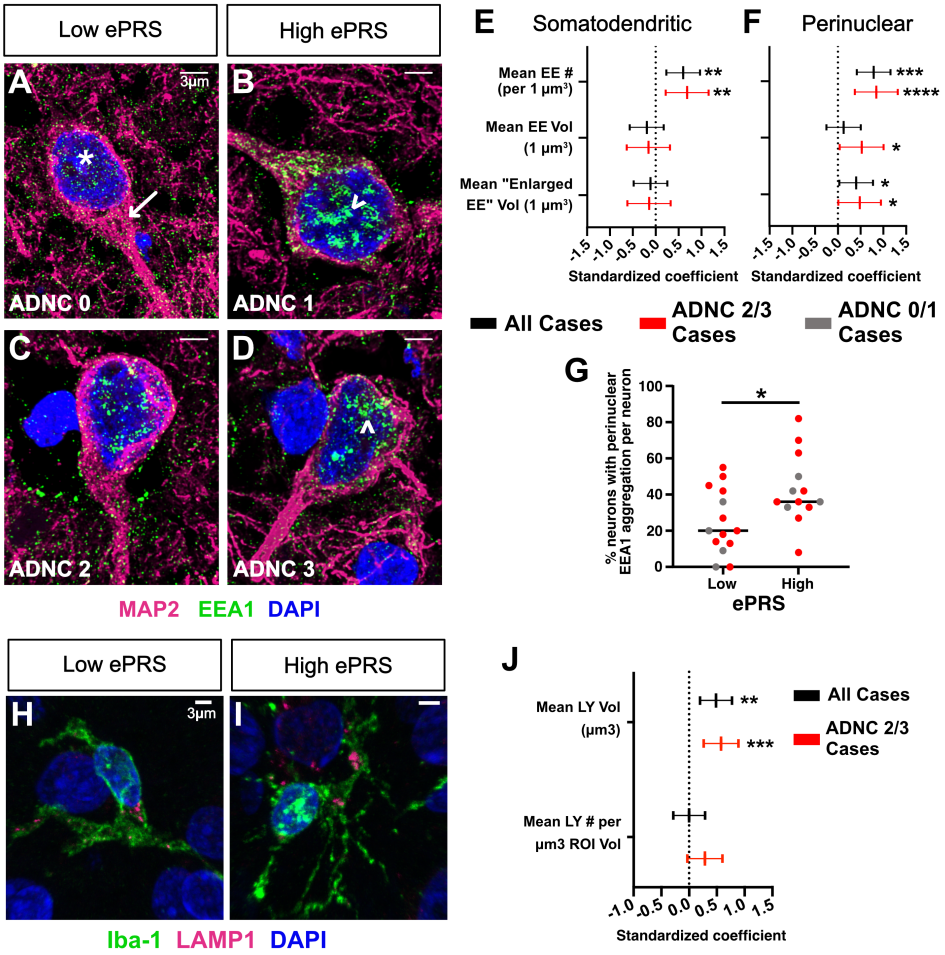
Low ePRS
High ePRS
A
3µm
B
ADNC 0
ADNC 1
C
D
ADNC 2
ADNC 3
MAP2 EEA1 DAPI
E Somatodendritic
F Perinuclear
Mean EE # (per 1 µm³)
Mean EE Vol (1 µm³)
Mean "Enlarged EE" Vol (1 µm³)
Standardized coefficient
All Cases
ADNC 2/3 Cases
ADNC 0/1 Cases
G
% neurons with perinuclear EEA1 aggregation per neuron
Low
High
ePRS
Low ePRS
High ePRS
H
3µm
I
Iba-1 LAMP1 DAPI
J
Mean LY Vol (µm3)
Mean LY # per µm3 ROI Vol
All Cases
ADNC 2/3 Cases
Standardized coefficient

Figure 3

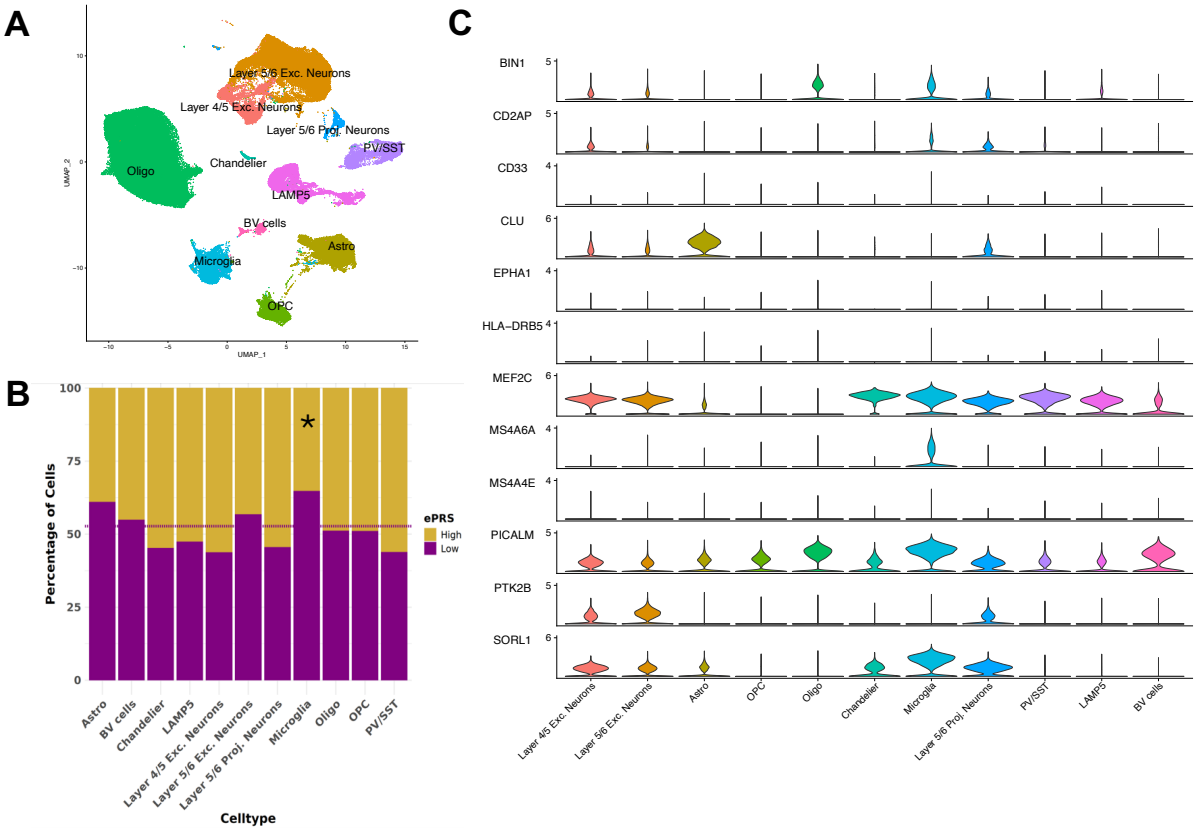
A
Layer 5/6 Exc. Neurons
Layer 4/5 Exc. Neurons
Layer 5/6 Proj. Neurons
PV/SST
Chandelier
Oligo
LAMP5
BV cells
Astro
Microglia
OPC
UMAP_1
UMAP_2
B
Percentage of Cells
ePRS
High
Low
Astro
BV cells
Chandelier
LAMP5
Layer 4/5 Exc. Neurons
Layer 5/6 Exc. Neurons
Layer 5/6 Proj. Neurons
Microglia
Oligo
OPC
PV/SST
Celltype
C
BIN1
CD2AP
CD33
CLU
EPHA1
HLA-DRB5
MEF2C
MS4A6A
MS4A4E
PICALM
PTK2B
SORL1
Layer 4/5 Exc. Neurons
Layer 5/6 Exc. Neurons
Astro
OPC
Oligo
Chandelier
Microglia
Layer 5/6 Proj. Neurons
PV/SST
LAMP5
BV cells

Figure 4

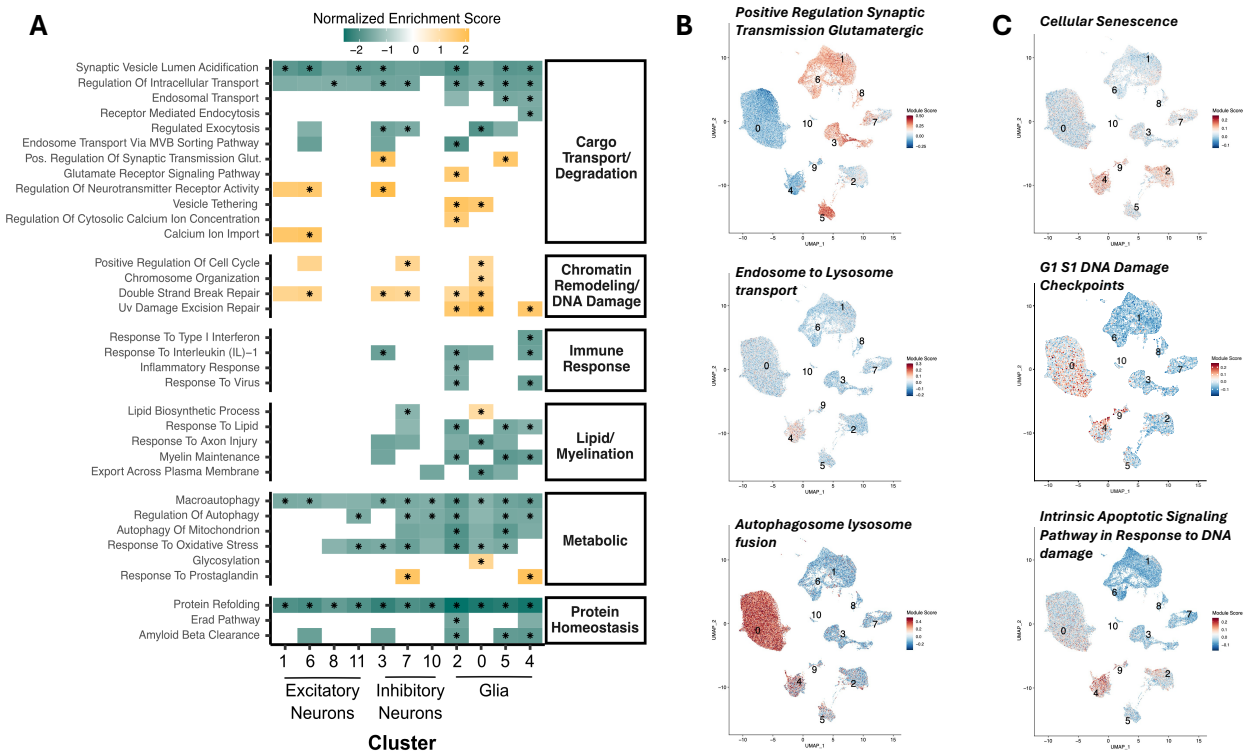
A
Normalized Enrichment Score
−2 −1 0 1 2
Synaptic Vesicle Lumen Acidification
Regulation Of Intracellular Transport
Endosomal Transport
Receptor Mediated Endocytosis
Regulated Exocytosis
Endosome Transport Via MVB Sorting Pathway
Pos. Regulation Of Synaptic Transmission Glut.
Glutamate Receptor Signaling Pathway
Regulation Of Neurotransmitter Receptor Activity
Vesicle Tethering
Regulation Of Cytosolic Calcium Ion Concentration
Calcium Ion Import
Cargo Transport/ Degradation
Positive Regulation Of Cell Cycle
Chromosome Organization
Double Strand Break Repair
Uv Damage Excision Repair
Chromatin Remodeling/ DNA Damage
Response To Type I Interferon
Response To Interleukin (IL)−1
Inflammatory Response
Response To Virus
Immune Response
Lipid Biosynthetic Process
Response To Lipid
Response To Axon Injury
Myelin Maintenance
Export Across Plasma Membrane
Lipid/ Myelination
Macroautophagy
Regulation Of Autophagy
Autophagy Of Mitochondrion
Response To Oxidative Stress
Glycosylation
Response To Prostaglandin
Metabolic
Protein Refolding
Erad Pathway
Amyloid Beta Clearance
Protein Homeostasis
1 6 8 11 3 7 10 2 0 5 4
Excitatory Neurons
Inhibitory Neurons
Glia
Cluster
B
Positive Regulation Synaptic Transmission Glutamatergic
Endosome to Lysosome transport
Autophagosome lysosome fusion
C
Cellular Senescence
G1 S1 DNA Damage Checkpoints
Intrinsic Apoptotic Signaling Pathway in Response to DNA damage

Figure 5

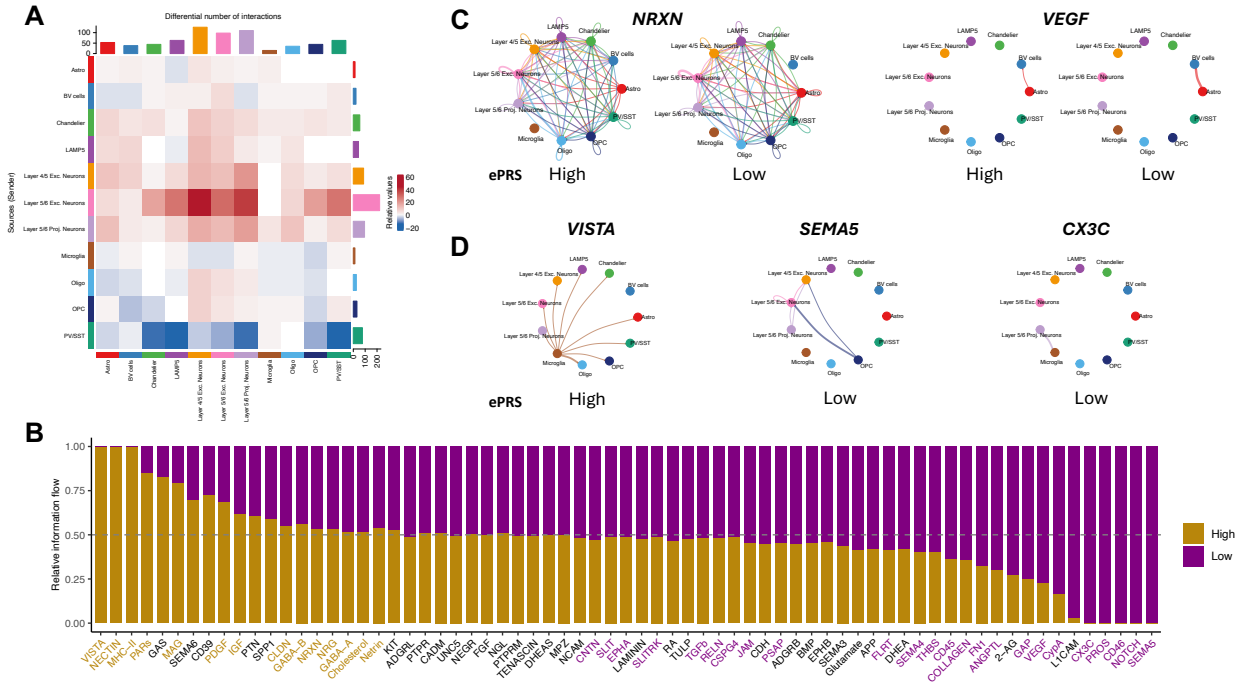
A
Differential number of interactions
Sources (Sender)
Relative values
B
Relative information flow
High
Low
C
NRXN
VEGF
ePRS
High
Low
D
VISTA
SEMA5
CX3C
ePRS
High
Low

Figure 6

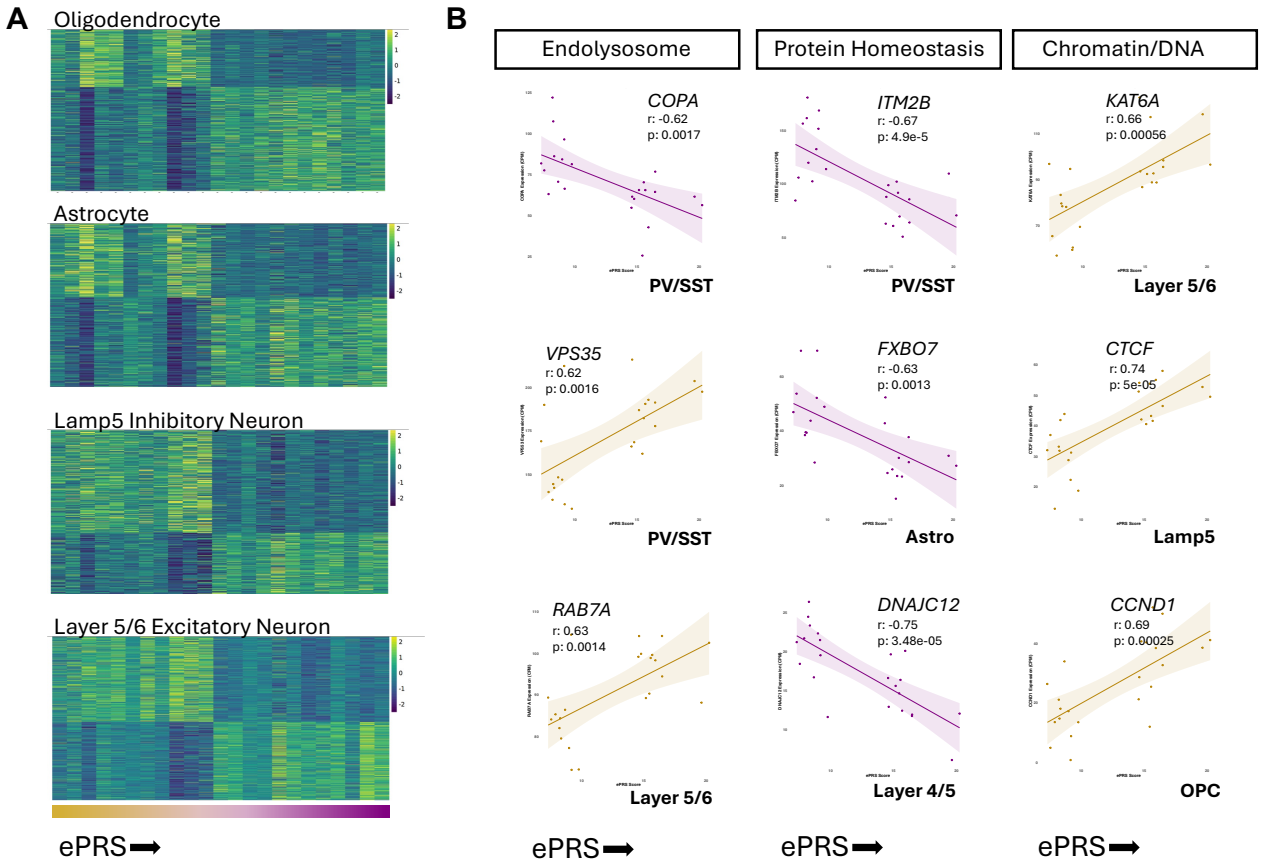
A
Oligodendrocyte
Astrocyte
Lamp5 Inhibitory Neuron
Layer 5/6 Excitatory Neuron
ePRS
B
Endolysosome
Protein Homeostasis
Chromatin/DNA
COPA
r: -0.62
p: 0.0017
PV/SST
ITM2B
r: -0.67
p: 4.9e-5
PV/SST
KAT6A
r: 0.66
p: 0.00056
Layer 5/6
VPS35
r: 0.62
p: 0.0016
PV/SST
FXBO7
r: -0.63
p: 0.0013
Astro
CTCF
r: 0.74
p: 5e-05
Lamp5
RAB7A
r: 0.63
p: 0.0014
Layer 5/6
DNAJC12
r: -0.75
p: 3.48e-05
Layer 4/5
CCND1
r: 0.69
p: 0.00025
OPC
ePRS
ePRS
ePRS
ePRS

[1] De Strooper B, Karran E: The Cellular Phase of Alzheimer's Disease. Cell 2016, 164:603-15.
[2] Lambert JC, Ibrahim-Verbaas CA, Harold D, Naj AC, Sims R, Bellenguez C, DeStafano AL, Bis JC, Beecham GW, Grenier-Boley B, Russo G, Thorton-Wells TA, Jones N, Smith AV, Chouraki V, Thomas C, Ikram MA, Zelenika D, Vardarajan BN, Kamatani Y, Lin CF, Gerrish A, Schmidt H, Kunkle B, Dunstan ML, Ruiz A, Bihoreau MT, Choi SH, Reitz C, Pasquier F, Cruchaga C, Craig D, Amin N, Berr C, Lopez OL, De Jager PL, Deramecourt V, Johnston JA, Evans D, Lovestone S, Letenneur L, Moron FJ, Rubinsztein DC, Eiriksdottir G, Sleegers K, Goate AM, Fievet N, Huentelman MW, Gill M, Brown K, Kamboh MI, Keller L, Barberger-Gateau P, McGuiness B, Larson EB, Green R, Myers AJ, Dufouil C, Todd S, Wallon D, Love S, Rogaeva E, Gallacher J, St George-Hyslop P, Clarimon J, Lleo A, Bayer A, Tsuang DW, Yu L, Tsolaki M, Bossu P, Spalletta G, Proitsi P, Collinge J, Sorbi S, Sanchez-Garcia F, Fox NC, Hardy J, Deniz Naranjo MC, Bosco P, Clarke R, Brayne C, Galimberti D, Mancuso M, Matthews F, European Alzheimer's Disease I, Genetic, Environmental Risk in Alzheimer's D, Alzheimer's Disease Genetic C, Cohorts for H, Aging Research in Genomic E, Moebus S, Mecocci P, Del Zompo M, Maier W, Hampel H, Pilotto A, Bullido M, Panza F, Caffarra P, Nacmias B, Gilbert JR, Mayhaus M, Lannefelt L, Hakonarson H, Pichler S, Carrasquillo MM, Ingelsson M, Beekly D, Alvarez V, Zou F, Valladares O, Younkin SG, Coto E, Hamilton-Nelson KL, Gu W, Razquin C, Pastor P, Mateo I, Owen MJ, Faber KM, Jonsson PV, Combarros O, O'Donovan MC, Cantwell LB, Soininen H, Blacker D, Mead S, Mosley TH, Jr., Bennett DA, Harris TB, Fratiglioni L, Holmes C, de Bruijn RF, Passmore P, Montine TJ, Bettens K, Rotter JI, Brice A, Morgan K, Foroud TM, Kukull WA, Hannequin D, Powell JF, Nalls MA, Ritchie K, Lunetta KL, Kauwe JS, Boerwinkle E, Riemenschneider M, Boada M, Hiltuenen M, Martin ER, Schmidt R, Rujescu D, Wang LS, Dartigues JF, Mayeux R, Tzourio C, Hofman A, Nothen MM, Graff C, Psaty BM, Jones L, Haines JL, Holmans PA, Lathrop M, Pericak-Vance MA, Launer LJ, Farrer LA, van Duijn CM, Van Broeckhoven C, Moskvina V, Seshadri S, Williams J, Schellenberg GD, Amouyel P: Meta-analysis of 74,046 individuals identifies 11 new susceptibility loci for Alzheimer's disease. Nat Genet 2013, 45:1452-8.
[3] Kunkle BW, Grenier-Boley B, Sims R, Bis JC, Damotte V, Naj AC, Boland A, Vronskaya M, van der Lee SJ, Amlie-Wolf A, Bellenguez C, Frizatti A, Chouraki V, Martin ER, Sleegers K, Badarinarayan N, Jakobsdottir J, Hamilton-Nelson KL, Moreno-Grau S, Olaso R, Raybould R, Chen Y, Kuzma AB, Hiltunen M, Morgan T, Ahmad S, Vardarajan BN, Epelbaum J, Hoffmann P, Boada M, Beecham GW, Garnier JG, Harold D, Fitzpatrick AL, Valladares O, Moutet ML, Gerrish A, Smith AV, Qu L, Bacq D, Denning N, Jian X, Zhao Y, Del Zompo M, Fox NC, Choi SH, Mateo I, Hughes JT, Adams HH, Malamon J, Sanchez-Garcia F, Patel Y, Brody JA, Dombroski BA, Naranjo MCD, Daniilidou M, Eiriksdottir G, Mukherjee S, Wallon D, Uphill J, Aspelund T, Cantwell LB, Garzia F, Galimberti D, Hofer E, Butkiewicz M, Fin B, Scarpini E, Sarnowski C, Bush WS, Meslage S, Kornhuber J, White CC, Song Y, Barber RC, Engelborghs S, Sordon S, Voijnovic D, Adams PM, Vandenberghe R, Mayhaus M, Cupples LA, Albert MS, De Deyn PP, Gu W, Himali JJ, Beekly D, Squassina A, Hartmann AM, Orellana A, Blacker D, Rodriguez-Rodriguez E, Lovestone S, Garcia ME, Doody RS, Munoz-Fernadez C, Sussams R, Lin H, Fairchild TJ, Benito YA, Holmes C, Karamujic-Comic H, Frosch MP, Thonberg H, Maier W, Roshchupkin G, Ghetti B, Giedraitis V, Kawalia A, Li S, Huebinger RM, Kilander L, Moebus S, Hernandez I, Kamboh MI, Brundin R, Turton J, Yang Q, Katz MJ, Concari L, Lord J, Beiser

AS, Keene CD, Helisalmi S, Kloszewska I, Kukull WA, Koivisto AM, Lynch A, Tarraga L, Larson EB, Haapasalo A, Lawlor B, Mosley TH, Lipton RB, Solfrizzi V, Gill M, Longstreth WT, Jr., Montine TJ, Frisardi V, Diez-Fairen M, Rivadeneira F, Petersen RC, Deramecourt V, Alvarez I, Salani F, Ciaramella A, Boerwinkle E, Reiman EM, Fievet N, Rotter JI, Reisch JS, Hanon O, Cupidi C, Andre Uitterlinden AG, Royall DR, Dufouil C, Maletta RG, de Rojas I, Sano M, Brice A, Cecchetti R, George-Hyslop PS, Ritchie K, Tsolaki M, Tsuang DW, Dubois B, Craig D, Wu CK, Soininen H, Avramidou D, Albin RL, Fratiglioni L, Germanou A, Apostolova LG, Keller L, Koutroumani M, Arnold SE, Panza F, Gkatzima O, Asthana S, Hannequin D, Whitehead P, Atwood CS, Caffarra P, Hampel H, Quintela I, Carracedo A, Lannfelt L, Rubinsztein DC, Barnes LL, Pasquier F, Frolich L, Barral S, McGuinness B, Beach TG, Johnston JA, Becker JT, Passmore P, Bigio EH, Schott JM, Bird TD, Warren JD, Boeve BF, Lupton MK, Bowen JD, Proitsi P, Boxer A, Powell JF, Burke JR, Kauwe JSK, Burns JM, Mancuso M, Buxbaum JD, Bonuccelli U, Cairns NJ, McQuillin A, Cao C, Livingston G, Carlson CS, Bass NJ, Carlsson CM, Hardy J, Carney RM, Bras J, Carrasquillo MM, Guerreiro R, Allen M, Chui HC, Fisher E, Masullo C, Crocco EA, DeCarli C, Bisceglio G, Dick M, Ma L, Duara R, Graff-Radford NR, Evans DA, Hodges A, Faber KM, Scherer M, Fallon KB, Riemenschneider M, Fardo DW, Heun R, Farlow MR, Kolsch H, Ferris S, Leber M, Foroud TM, Heuser I, Galasko DR, Giegling I, Gearing M, Hull M, Geschwind DH, Gilbert JR, Morris J, Green RC, Mayo K, Growdon JH, Feulner T, Hamilton RL, Harrell LE, Drichel D, Honig LS, Cushion TD, Huentelman MJ, Hollingworth P, Hulette CM, Hyman BT, Marshall R, Jarvik GP, Meggy A, Abner E, Menzies GE, Jin LW, Leonenko G, Real LM, Jun GR, Baldwin CT, Grozeva D, Karydas A, Russo G, Kaye JA, Kim R, Jessen F, Kowall NW, Vellas B, Kramer JH, Vardy E, LaFerla FM, Jockel KH, Lah JJ, Dichgans M, Leverenz JB, Mann D, Levey AI, Pickering-Brown S, Lieberman AP, Klopp N, Lunetta KL, Wichmann HE, Lyketsos CG, Morgan K, Marson DC, Brown K, Martiniuk F, Medway C, Mash DC, Nothen MM, Masliah E, Hooper NM, McCormick WC, Daniele A, McCurry SM, Bayer A, McDavid AN, Gallacher J, McKee AC, van den Bussche H, Mesulam M, Brayne C, Miller BL, Riedel-Heller S, Miller CA, Miller JW, Al-Chalabi A, Morris JC, Shaw CE, Myers AJ, Wiltfang J, O'Bryant S, Olichney JM, Alvarez V, Parisi JE, Singleton AB, Paulson HL, Collinge J, Perry WR, Mead S, Peskind E, Cribbs DH, Rossor M, Pierce A, Ryan NS, Poon WW, Nacmias B, Potter H, Sorbi S, Quinn JF, Sacchinelli E, Raj A, Spalletta G, Raskind M, Caltagirone C, Bossu P, Orfei MD, Reisberg B, Clarke R, Reitz C, Smith AD, Ringman JM, Warden D, Roberson ED, Wilcock G, Rogaeva E, Bruni AC, Rosen HJ, Gallo M, Rosenberg RN, Ben-Shlomo Y, Sager MA, Mecocci P, Saykin AJ, Pastor P, Cuccaro ML, Vance JM, Schneider JA, Schneider LS, Slifer S, Seeley WW, Smith AG, Sonnen JA, Spina S, Stern RA, Swerdlow RH, Tang M, Tanzi RE, Trojanowski JQ, Troncoso JC, Van Deerlin VM, Van Eldik LJ, Vinters HV, Vonsattel JP, Weintraub S, Welsh-Bohmer KA, Wilhelmsen KC, Williamson J, Wingo TS, Woltjer RL, Wright CB, Yu CE, Yu L, Saba Y, Pilotto A, Bullido MJ, Peters O, Crane PK, Bennett D, Bosco P, Coto E, Boccardi V, De Jager PL, Lleo A, Warner N, Lopez OL, Ingelsson M, Deloukas P, Cruchaga C, Graff C, Gwilliam R, Fornage M, Goate AM, Sanchez-Juan P, Kehoe PG, Amin N, Ertekin-Taner N, Berr C, Debette S, Love S, Launer LJ, Younkin SG, Dartigues JF, Corcoran C, Ikram MA, Dickson DW, Nicolas G, Campion D, Tschanz J, Schmidt H, Hakonarson H, Clarimon J, Munger R, Schmidt R, Farrer LA, Van Broeckhoven C, M COD, DeStefano AL, Jones L, Haines JL, Deleuze JF, Owen MJ, Gudnason V, Mayeux R, Escott-Price V, Psaty BM, Ramirez A, Wang LS, Ruiz A, van Duijn CM, Holmans PA, Seshadri S, Williams J, Amouyel P, Schellenberg GD,

Lambert JC, Pericak-Vance MA, Alzheimer Disease Genetics C, European Alzheimer's Disease I, Cohorts for H, Aging Research in Genomic Epidemiology C, Genetic, Environmental Risk in Ad/Defining Genetic P, Environmental Risk for Alzheimer's Disease C: Genetic meta-analysis of diagnosed Alzheimer's disease identifies new risk loci and implicates Abeta, tau, immunity and lipid processing. Nat Genet 2019, 51:414-30.
[4] Jansen IE, Savage JE, Watanabe K, Bryois J, Williams DM, Steinberg S, Sealock J, Karlsson IK, Hagg S, Athanasiu L, Voyle N, Proitsi P, Witoelar A, Stringer S, Aarsland D, Almdahl IS, Andersen F, Bergh S, Bettella F, Bjornsson S, Braekhus A, Brathen G, de Leeuw C, Desikan RS, Djurovic S, Dumitrescu L, Fladby T, Hohman TJ, Jonsson PV, Kiddle SJ, Rongve A, Saltvedt I, Sando SB, Selbaek G, Shoai M, Skene NG, Snaedal J, Stordal E, Ulstein ID, Wang Y, White LR, Hardy J, Hjerling-Leffler J, Sullivan PF, van der Flier WM, Dobson R, Davis LK, Stefansson H, Stefansson K, Pedersen NL, Ripke S, Andreassen OA, Posthuma D: Genome-wide meta-analysis identifies new loci and functional pathways influencing Alzheimer's disease risk. Nat Genet 2019, 51:404-13.
[5] de Rojas I, Moreno-Grau S, Tesi N, Grenier-Boley B, Andrade V, Jansen IE, Pedersen NL, Stringa N, Zettergren A, Hernandez I, Montrreal L, Antunez C, Antonell A, Tankard RM, Bis JC, Sims R, Bellenguez C, Quintela I, Gonzalez-Perez A, Calero M, Franco-Macias E, Macias J, Blesa R, Cervera-Carles L, Menendez-Gonzalez M, Frank-Garcia A, Royo JL, Moreno F, Huerto Vilas R, Baquero M, Diez-Fairen M, Lage C, Garcia-Madrona S, Garcia-Gonzalez P, Alarcon-Martin E, Valero S, Sotolongo-Grau O, Ullgren A, Naj AC, Lemstra AW, Benaque A, Perez-Cordon A, Benussi A, Rabano A, Padovani A, Squassina A, de Mendonca A, Arias Pastor A, Kok AAL, Meggy A, Pastor AB, Espinosa A, Corma-Gomez A, Martin Montes A, Sanabria A, DeStefano AL, Schneider A, Haapasalo A, Kinhult Stahlbom A, Tybjaerg-Hansen A, Hartmann AM, Spottke A, Corbaton-Anchuelo A, Rongve A, Borroni B, Arosio B, Nacmias B, Nordestgaard BG, Kunkle BW, Charbonnier C, Abdelnour C, Masullo C, Martinez Rodriguez C, Munoz-Fernandez C, Dufouil C, Graff C, Ferreira CB, Chillotti C, Reynolds CA, Fenoglio C, Van Broeckhoven C, Clark C, Pisanu C, Satizabal CL, Holmes C, Buiza-Rueda D, Aarsland D, Rujescu D, Alcolea D, Galimberti D, Wallon D, Seripa D, Grunblatt E, Dardiotis E, Duzel E, Scarpini E, Conti E, Rubino E, Gelpi E, Rodriguez-Rodriguez E, Duron E, Boerwinkle E, Ferri E, Tagliavini F, Kucukali F, Pasquier F, Sanchez-Garcia F, Mangialasche F, Jessen F, Nicolas G, Selbaek G, Ortega G, Chene G, Hadjigeorgiou G, Rossi G, Spalletta G, Giaccone G, Grande G, Binetti G, Papenberg G, Hampel H, Bailly H, Zetterberg H, Soininen H, Karlsson IK, Alvarez I, Appollonio I, Giegling I, Skoog I, Saltvedt I, Rainero I, Rosas Allende I, Hort J, Diehl-Schmid J, Van Dongen J, Vidal JS, Lehtisalo J, Wiltfang J, Thomassen JQ, Kornhuber J, Haines JL, Vogelgsang J, Pineda JA, Fortea J, Popp J, Deckert J, Buerger K, Morgan K, Fliessbach K, Sleegers K, Molina-Porcel L, Kilander L, Weinhold L, Farrer LA, Wang LS, Kleineidam L, Farotti L, Parnetti L, Tremolizzo L, Hausner L, Benussi L, Froelich L, Ikram MA, Deniz-Naranjo MC, Tsolaki M, Rosende-Roca M, Lowenmark M, Hulsman M, Spallazzi M, Pericak-Vance MA, Esiri M, Bernal Sanchez-Arjona M, Dalmasso MC, Martinez-Larrad MT, Arcaro M, Nothen MM, Fernandez-Fuertes M, Dichgans M, Ingelsson M, Herrmann MJ, Scherer M, Vyhnalek M, Kosmidis MH, Yannakoulia M, Schmid M, Ewers M, Heneka MT, Wagner M, Scamosci M, Kivipelto M, Hiltunen M, Zulaica M, Alegret M, Fornage M, Roberto N, van Schoor NM, Seidu NM, Banaj N, Armstrong NJ, Scarmeas N, Scherbaum N, Goldhardt O, Hanon O, Peters O, Skrobot OA, Quenez O, Lerch O, Bossu P, Caffarra P, Dionigi Rossi P,

Sakka P, Mecocci P, Hoffmann P, Holmans PA, Fischer P, Riederer P, Yang Q, Marshall R, Kalaria RN, Mayeux R, Vandenberghe R, Cecchetti R, Ghidoni R, Frikke-Schmidt R, Sorbi S, Hagg S, Engelborghs S, Helisalmi S, Botne Sando S, Kern S, Archetti S, Boschi S, Fostinelli S, Gil S, Mendoza S, Mead S, Ciccone S, Djurovic S, Heilmann-Heimbach S, Riedel-Heller S, Kuulasmaa T, Del Ser T, Lebouvier T, Polak T, Ngandu T, Grimmer T, Bessi V, Escott-Price V, Giedraitis V, Deramecourt V, Maier W, Jian X, Pijnenburg YAL, contributors E, group GAs, consortium D, Igap, consortia P-A, Kehoe PG, Garcia-Ribas G, Sanchez-Juan P, Pastor P, Perez-Tur J, Pinol-Ripoll G, Lopez de Munain A, Garcia-Alberca JM, Bullido MJ, Alvarez V, Lleo A, Real LM, Mir P, Medina M, Scheltens P, Holstege H, Marquie M, Saez ME, Carracedo A, Amouyel P, Schellenberg GD, Williams J, Seshadri S, van Duijn CM, Mather KA, Sanchez-Valle R, Serrano-Rios M, Orellana A, Tarraga L, Blennow K, Huisman M, Andreassen OA, Posthuma D, Clarimon J, Boada M, van der Flier WM, Ramirez A, Lambert JC, van der Lee SJ, Ruiz A: Common variants in Alzheimer's disease and risk stratification by polygenic risk scores. Nat Commun 2021, 12:3417.

[6] Bellenguez Cea: New insights on the genetic etiology of Alzheimer's and related dementia. medRxiv 2020, doi.org/10.1101/2020.10.0120200659.

[7] Bellou E, Kim W, Leonenko G, Tao F, Simmonds E, Wu Y, Mattsson-Carlgren N, Hansson O, Nagle MW, Escott-Price V, Alzheimer's Disease Neuroimaging I: Benchmarking Alzheimer's disease prediction: personalised risk assessment using polygenic risk scores across various methodologies and genome-wide studies. Alzheimers Res Ther 2025, 17:6.

[8] Che R, Motsinger-Reif AA: A new explained-variance based genetic risk score for predictive modeling of disease risk. Stat Appl Genet Mol Biol 2012, 11:Article 15.

[9] Clark K, Leung YY, Lee WP, Voight B, Wang LS: Polygenic Risk Scores in Alzheimer's Disease Genetics: Methodology, Applications, Inclusion, and Diversity. J Alzheimers Dis 2022, 89:1-12.

[10] Xu Y, Vasiljevic E, Deming YK, Jonaitis EM, Koscik RL, Van Hulle CA, Lu Q, Carboni M, Kollmorgen G, Wild N, Carlsson CM, Johnson SC, Zetterberg H, Blennow K, Engelman CD: Effect of Pathway-Specific Polygenic Risk Scores for Alzheimer's Disease (AD) on Rate of Change in Cognitive Function and AD-Related Biomarkers Among Asymptomatic Individuals. J Alzheimers Dis 2023, 94:1587-605.

[11] Tesi N, van der Lee SJ, Hulsman M, Jansen IE, Stringa N, van Schoor NM, Scheltens P, van der Flier WM, Huisman M, Reinders MJT, Holstege H: Immune response and endocytosis pathways are associated with the resilience against Alzheimer's disease. Transl Psychiatry 2020, 10:332.

[12] Sun Y, Wang M, Zhao Y, Hu K, Liu Y, Liu B, Alzheimer's Disease Neuroimaging I: A Pathway-Specific Polygenic Risk Score Is Associated with Tau Pathology and Cognitive Decline. J Alzheimers Dis 2022, 85:1745-54.

[13] Schork NJ, Elman JA, Alzheimer's Disease Neuroimaging I: Pathway-Specific Polygenic Risk Scores Correlate with Clinical Status and Alzheimer's Disease-Related Biomarkers. J Alzheimers Dis 2023, 95:915-29.

[14] Femminella GD, Harold D, Scott J, Williams J, Edison P, Alzheimer's Disease Neuroimaging I: The Differential Influence of Immune, Endocytotic, and Lipid Metabolism Genes on Amyloid Deposition and Neurodegeneration in Subjects at Risk of Alzheimer's Disease. J Alzheimers Dis 2021, 79:127-39.

[15] Escott-Price V, Myers AJ, Huentelman M, Hardy J: Polygenic risk score analysis of pathologically confirmed Alzheimer disease. Ann Neurol 2017, 82:311-4.
[16] Darst BF, Koscik RL, Racine AM, Oh JM, Krause RA, Carlsson CM, Zetterberg H, Blennow K, Christian BT, Bendlin BB, Okonkwo OC, Hogan KJ, Hermann BP, Sager MA, Asthana S, Johnson SC, Engelman CD: Pathway-Specific Polygenic Risk Scores as Predictors of Amyloid-beta Deposition and Cognitive Function in a Sample at Increased Risk for Alzheimer's Disease. J Alzheimers Dis 2017, 55:473-84.
[17] Ahmad S, Bannister C, van der Lee SJ, Vojinovic D, Adams HHH, Ramirez A, Escott-Price V, Sims R, Baker E, Williams J, Holmans P, Vernooij MW, Ikram MA, Amin N, van Duijn CM: Disentangling the biological pathways involved in early features of Alzheimer's disease in the Rotterdam Study. Alzheimers Dement 2018, 14:848-57.
[18] Karch CM, Goate AM: Alzheimer's disease risk genes and mechanisms of disease pathogenesis. Biol Psychiatry 2015, 77:43-51.
[19] Szabo MP, Mishra S, Knupp A, Young JE: The role of Alzheimer's disease risk genes in endolysosomal pathways. Neurobiol Dis 2022, 162:105576.
[20] Van Acker ZP, Bretou M, Annaert W: Endo-lysosomal dysregulations and late-onset Alzheimer's disease: impact of genetic risk factors. Mol Neurodegener 2019, 14:20.
[21] Young JE, Holstege H, Andersen OM, Petsko GA, Small SA: On the causal role of retromer-dependent endosomal recycling in Alzheimer's disease. Nat Cell Biol 2023, 25:1394-7.
[22] Xue D, Blue EE, Sofer T, Hughes TM, Rotter JI, Fohner AE: Polygenic risk scores for incident dementia in the Multi-Ethnic Study of Atherosclerosis. Genet Epidemiol submitted 2025.
[23] Sleegers K, Bettens K, De Roeck A, Van Cauwenberghe C, Cuyvers E, Verheijen J, Struyfs H, Van Dongen J, Vermeulen S, Engelborghs S, Vandenbulcke M, Vandenberghe R, De Deyn PP, Van Broeckhoven C, consortium B: A 22-single nucleotide polymorphism Alzheimer's disease risk score correlates with family history, onset age, and cerebrospinal fluid Abeta42. Alzheimers Dement 2015, 11:1452-60.
[24] Van Cauwenberghe C, Van Broeckhoven C, Sleegers K: The genetic landscape of Alzheimer disease: clinical implications and perspectives. Genet Med 2016, 18:421-30.
[25] Cataldo AM, Peterhoff CM, Troncoso JC, Gomez-Isla T, Hyman BT, Nixon RA: Endocytic pathway abnormalities precede amyloid beta deposition in sporadic Alzheimer's disease and Down syndrome: differential effects of APOE genotype and presenilin mutations. Am J Pathol 2000, 157:277-86.
[26] Kwart D, Gregg A, Scheckel C, Murphy EA, Paquet D, Duffield M, Fak J, Olsen O, Darnell RB, Tessier-Lavigne M: A Large Panel of Isogenic APP and PSEN1 Mutant Human iPSC Neurons Reveals Shared Endosomal Abnormalities Mediated by APP beta-CTFs, Not Abeta. Neuron 2019, 104:256-70 e5.
[27] Lee JH, Yang DS, Goulbourne CN, Im E, Stavrides P, Pensalfini A, Chan H, Bouchet-Marquis C, Bleiwas C, Berg MJ, Huo C, Peddy J, Pawlik M, Levy E, Rao M, Staufenbiel M, Nixon RA: Faulty autolysosome acidification in Alzheimer's disease mouse models induces autophagic build-up of Abeta in neurons, yielding senile plaques. Nat Neurosci 2022, 25:688-701.

[28] Knupp A, Mishra S, Martinez R, Braggin JE, Szabo M, Kinoshita C, Hailey DW, Small SA, Jayadev S, Young JE: Depletion of the AD Risk Gene SORL1 Selectively Impairs Neuronal Endosomal Traffic Independent of Amyloidogenic APP Processing. Cell Rep 2020, 31:107719.
[29] Filippone A, Pratico D: Endosome Dysregulation in Down Syndrome: A Potential Contributor to Alzheimer Disease Pathology. Ann Neurol 2021, 90:4-14.
[30] Somogyi A, Kirkham ED, Lloyd-Evans E, Winston J, Allen ND, Mackrill JJ, Anderson KE, Hawkins PT, Gardiner SE, Waller-Evans H, Sims R, Boland B, O'Neill C: The synthetic TRPML1 agonist ML-SA1 rescues Alzheimer-related alterations of the endosomal-autophagic-lysosomal system. J Cell Sci 2023, 136.
[31] Lee H, Aylward AJ, Pearse RV, 2nd, Lish AM, Hsieh YC, Augur ZM, Benoit CR, Chou V, Knupp A, Pan C, Goberdhan S, Duong DM, Seyfried NT, Bennett DA, Taga MF, Huynh K, Arnold M, Meikle PJ, De Jager PL, Menon V, Young JE, Young-Pearse TL: Cell-type-specific regulation of APOE and CLU levels in human neurons by the Alzheimer's disease risk gene SORL1. Cell Rep 2023, 42:112994.
[32] Emani PS, Liu JJ, Clarke D, Jensen M, Warrell J, Gupta C, Meng R, Lee CY, Xu S, Dursun C, Lou S, Chen Y, Chu Z, Galeev T, Hwang A, Li Y, Ni P, Zhou X, Psych ECd, Bakken TE, Bendl J, Bicks L, Chatterjee T, Cheng L, Cheng Y, Dai Y, Duan Z, Flaherty M, Fullard JF, Gancz M, Garrido-Martin D, Gaynor-Gillett S, Grundman J, Hawken N, Henry E, Hoffman GE, Huang A, Jiang Y, Jin T, Jorstad NL, Kawaguchi R, Khullar S, Liu J, Liu J, Liu S, Ma S, Margolis M, Mazariegos S, Moore J, Moran JR, Nguyen E, Phalke N, Pjanic M, Pratt H, Quintero D, Rajagopalan AS, Riesenmy TR, Shedd N, Shi M, Spector M, Terwilliger R, Travaglini KJ, Wamsley B, Wang G, Xia Y, Xiao S, Yang AC, Zheng S, Gandal MJ, Lee D, Lein ES, Roussos P, Sestan N, Weng Z, White KP, Won H, Girgenti MJ, Zhang J, Wang D, Geschwind D, Gerstein M, Psych EC: Single-cell genomics and regulatory networks for 388 human brains. Science 2024, 384:eadi5199.
[33] Mathys H, Boix CA, Akay LA, Xia Z, Davila-Velderrain J, Ng AP, Jiang X, Abdelhady G, Galani K, Mantero J, Band N, James BT, Babu S, Galiana-Melendez F, Louderback K, Prokopenko D, Tanzi RE, Bennett DA, Tsai LH, Kellis M: Single-cell multiregion dissection of Alzheimer's disease. Nature 2024, 632:858-68.
[34] Mathys H, Davila-Velderrain J, Peng Z, Gao F, Mohammadi S, Young JZ, Menon M, He L, Abdurrob F, Jiang X, Martorell AJ, Ransohoff RM, Hafler BP, Bennett DA, Kellis M, Tsai LH: Single-cell transcriptomic analysis of Alzheimer's disease. Nature 2019, 570:332-7.
[35] Patsialou A, Wilsker D, Moran E: DNA-binding properties of ARID family proteins. Nucleic Acids Res 2005, 33:66-80.
[36] Asmar AJ, Abrams SR, Hsin J, Collins JC, Yazejian RM, Wu Y, Cho J, Doyle AD, Cinthala S, Simon M, van Jaarsveld RH, Beck DB, Kerosuo L, Werner A: A ubiquitin-based effector-to-inhibitor switch coordinates early brain, craniofacial, and skin development. Nat Commun 2023, 14:4499.
[37] Yoast RE, Emrich SM, Zhang X, Xin P, Johnson MT, Fike AJ, Walter V, Hempel N, Yule DI, Sneyd J, Gill DL, Trebak M: The native ORAI channel trio underlies the diversity of Ca(2+) signaling events. Nat Commun 2020, 11:2444.

[38] Gu X, Mao X, Lussier MP, Hutchison MA, Zhou L, Hamra FK, Roche KW, Lu W: GSG1L suppresses AMPA receptor-mediated synaptic transmission and uniquely modulates AMPA receptor kinetics in hippocampal neurons. Nat Commun 2016, 7:10873.
[39] Arons MH, Lee K, Thynne CJ, Kim SA, Schob C, Kindler S, Montgomery JM, Garner CC: Shank3 Is Part of a Zinc-Sensitive Signaling System That Regulates Excitatory Synaptic Strength. J Neurosci 2016, 36:9124-34.
[40] Eltokhi A, Gonzalez-Lozano MA, Oettl LL, Rozov A, Pitzer C, Roth R, Berkel S, Huser M, Harten A, Kelsch W, Smit AB, Rappold GA, Sprengel R: Imbalanced post- and extrasynaptic SHANK2A functions during development affect social behavior in SHANK2-mediated neuropsychiatric disorders. Mol Psychiatry 2021, 26:6482-504.
[41] Lipstein N, Verhoeven-Duif NM, Michelassi FE, Calloway N, van Hasselt PM, Pienkowska K, van Haaften G, van Haelst MM, van Empelen R, Cuppen I, van Teeseling HC, Evelein AM, Vorstman JA, Thoms S, Jahn O, Duran KJ, Monroe GR, Ryan TA, Taschenberger H, Dittman JS, Rhee JS, Visser G, Jans JJ, Brose N: Synaptic UNC13A protein variant causes increased neurotransmission and dyskinetic movement disorder. J Clin Invest 2017, 127:1005-18.
[42] Dupuis JP, Nicole O, Groc L: NMDA receptor functions in health and disease: Old actor, new dimensions. Neuron 2023, 111:2312-28.
[43] Qneibi M, Bdir S, Bdair M, Aldwaik SA, Heeh M, Sandouka D, Idais T: Exploring the role of AMPA receptor auxiliary proteins in synaptic functions and diseases. FEBS J 2024.
[44] Bergles DE, Roberts JD, Somogyi P, Jahr CE: Glutamatergic synapses on oligodendrocyte precursor cells in the hippocampus. Nature 2000, 405:187-91.
[45] Jordan KL, Koss DJ, Outeiro TF, Giorgini F: Therapeutic Targeting of Rab GTPases: Relevance for Alzheimer's Disease. Biomedicines 2022, 10.
[46] Anitei M, Cowan AE, Pfeiffer SE, Bansal R: Role for Rab3a in oligodendrocyte morphological differentiation. J Neurosci Res 2009, 87:342-52.
[47] Lam M, Takeo K, Almeida RG, Cooper MH, Wu K, Iyer M, Kantarci H, Zuchero JB: CNS myelination requires VAMP2/3-mediated membrane expansion in oligodendrocytes. Nat Commun 2022, 13:5583.
[48] Trajkovic K, Dhaunchak AS, Goncalves JT, Wenzel D, Schneider A, Bunt G, Nave KA, Simons M: Neuron to glia signaling triggers myelin membrane exocytosis from endosomal storage sites. J Cell Biol 2006, 172:937-48.
[49] Feldmann A, Amphornrat J, Schonherr M, Winterstein C, Mobius W, Ruhwedel T, Danglot L, Nave KA, Galli T, Bruns D, Trotter J, Kramer-Albers EM: Transport of the major myelin proteolipid protein is directed by VAMP3 and VAMP7. J Neurosci 2011, 31:5659-72.
[50] Jin S, Plikus MV, Nie Q: CellChat for systematic analysis of cell-cell communication from single-cell transcriptomics. Nat Protoc 2025, 20:180-219.
[51] Zhao W, Johnston KG, Ren H, Xu X, Nie Q: Inferring neuron-neuron communications from single-cell transcriptomics through NeuronChat. Nat Commun 2023, 14:1128.
[52] Steiner A, Hrovat-Schaale K, Prigione I, Yu CH, Laohamonthonkul P, Harapas CR, Low RRJ, De Nardo D, Dagley LF, Mlodzianoski MJ, Rogers KL, Zillinger T, Hartmann G, Gantier MP, Gattorno M, Geyer M, Volpi S, Davidson S, Masters SL: Deficiency in coatomer complex I causes aberrant activation of STING signalling. Nat Commun 2022, 13:2321.

[53] Choi J, Djebbar S, Fournier A, Labrie C: The co-chaperone DNAJC12 binds to Hsc70 and is upregulated by endoplasmic reticulum stress. Cell Stress Chaperones 2014, 19:439-46.
[54] Navarro E, Esteras N: A new mutation in the Parkinson's-related FBXO7 gene impairs mitochondrial and proteasomal function. FEBS J 2024, 291:2562-4.
[55] Wohlschlegel J, Argentini M, Michiels C, Letellier C, Forster V, Condroyer C, He Z, Thuret G, Zeitz C, Leger T, Audo I: First identification of ITM2B interactome in the human retina. Sci Rep 2021, 11:17210.
[56] Van Acker ZP, Perdok A, Bretou M, Annaert W: The microglial lysosomal system in Alzheimer's disease: Guardian against proteinopathy. Ageing Res Rev 2021, 71:101444.
[57] Winckler B, Faundez V, Maday S, Cai Q, Guimas Almeida C, Zhang H: The Endolysosomal System and Proteostasis: From Development to Degeneration. J Neurosci 2018, 38:9364-74.
[58] Wong CO: Endosomal-Lysosomal Processing of Neurodegeneration-Associated Proteins in Astrocytes. Int J Mol Sci 2020, 21.
[59] Young JE, Fong LK, Frankowski H, Petsko GA, Small SA, Goldstein LSB: Stabilizing the Retromer Complex in a Human Stem Cell Model of Alzheimer's Disease Reduces TAU Phosphorylation Independently of Amyloid Precursor Protein. Stem Cell Reports 2018, 10:1046-58.
[60] Hung C, Tuck E, Stubbs V, van der Lee SJ, Aalfs C, van Spaendonk R, Scheltens P, Hardy J, Holstege H, Livesey FJ: SORL1 deficiency in human excitatory neurons causes APP-dependent defects in the endolysosome-autophagy network. Cell Rep 2021, 35:109259.
[61] Saha O, Melo de Farias AR, Pelletier A, Siedlecki-Wullich D, Landeira BS, Gadaut J, Carrier A, Vreulx AC, Guyot K, Shen Y, Bonnefond A, Amouyel P, Tcw J, Kilinc D, Queiroz CM, Delahaye F, Lambert JC, Costa MR: The Alzheimer's disease risk gene BIN1 regulates activity-dependent gene expression in human-induced glutamatergic neurons. Mol Psychiatry 2024, 29:2634-46.
[62] Mishra S, Knupp A, Szabo MP, Williams CA, Kinoshita C, Hailey DW, Wang Y, Andersen OM, Young JE: The Alzheimer's gene SORL1 is a regulator of endosomal traffic and recycling in human neurons. Cell Mol Life Sci 2022, 79:162.
[63] Simoes S, Guo J, Buitrago L, Qureshi YH, Feng X, Kothiya M, Cortes E, Patel V, Kannan S, Kim YH, Chang KT, Alzheimer's Disease Neuroimaging I, Hussaini SA, Moreno H, Di Paolo G, Andersen OM, Small SA: Alzheimer's vulnerable brain region relies on a distinct retromer core dedicated to endosomal recycling. Cell Rep 2021, 37:110182.
[64] Temkin P, Morishita W, Goswami D, Arendt K, Chen L, Malenka R: The Retromer Supports AMPA Receptor Trafficking During LTP. Neuron 2017, 94:74-82 e5.
[65] de Araujo MEG, Liebscher G, Hess MW, Huber LA: Lysosomal size matters. Traffic 2020, 21:60-75.
[66] Prater KE, Green KJ, Mamde S, Sun W, Cochoit A, Smith CL, Chiou KL, Heath L, Rose SE, Wiley J, Keene CD, Kwon RY, Snyder-Mackler N, Blue EE, Logsdon B, Young JE, Shojaie A, Garden GA, Jayadev S: Human microglia show unique transcriptional changes in Alzheimer's disease. Nat Aging 2023.
[67] Fang LP, Lin CH, Medlej Y, Zhao R, Chang HF, Guo Q, Wu Z, Su Y, Zhao N, Gobbo D, Wyatt A, Wahl V, Fiore F, Tu SM, Boehm U, Huang W, Bian S, Agarwal A, Lauterbach MA, Yi

C, Niu J, Scheller A, Kirchhoff F, Bai X: Oligodendrocyte precursor cells facilitate neuronal lysosome release. Nat Commun 2025, 16:1175.
[68] Zhu SY, Yao RQ, Li YX, Zhao PY, Ren C, Du XH, Yao YM: Lysosomal quality control of cell fate: a novel therapeutic target for human diseases. Cell Death Dis 2020, 11:817.
[69] Lee WP, Choi SH, Shea MG, Cheng PL, Dombroski BA, Pitsillides AN, Heard-Costa NL, Wang H, Bulekova K, Kuzma AB, Leung YY, Farrell JJ, Lin H, Naj A, Blue EE, Nusetor F, Wang D, Boerwinkle E, Bush WS, Zhang X, De Jager PL, Dupuis J, Farrer LA, Fornage M, Martin E, Pericak-Vance M, Seshadri S, Wijsman EM, Wang LS, Schellenberg GD, Destefano AL, Haines JL, Peloso GM: Association of Common and Rare Variants with Alzheimer's Disease in over 13,000 Diverse Individuals with Whole-Genome Sequencing from the Alzheimer's Disease Sequencing Project. medRxiv 2023.
[70] Filipello F, You SF, Mirfakhar FS, Mahali S, Bollman B, Acquarone M, Korvatska O, Marsh JA, Sivaraman A, Martinez R, Cantoni C, De Feo L, Ghezzi L, Minaya MA, Renganathan A, Cashikar AG, Satoh JI, Beatty W, Iyer AK, Cella M, Raskind WH, Piccio L, Karch CM: Defects in lysosomal function and lipid metabolism in human microglia harboring a TREM2 loss of function mutation. Acta Neuropathol 2023, 145:749-72.
[71] Genomes Project C, Auton A, Brooks LD, Durbin RM, Garrison EP, Kang HM, Korbel JO, Marchini JL, McCarthy S, McVean GA, Abecasis GR: A global reference for human genetic variation. Nature 2015, 526:68-74.
[72] Machiela MJ, Chanock SJ: LDlink: a web-based application for exploring population-specific haplotype structure and linking correlated alleles of possible functional variants. Bioinformatics 2015, 31:3555-7.
[73] Montine TJ, Phelps CH, Beach TG, Bigio EH, Cairns NJ, Dickson DW, Duyckaerts C, Frosch MP, Masliah E, Mirra SS, Nelson PT, Schneider JA, Thal DR, Trojanowski JQ, Vinters HV, Hyman BT, National Institute on A, Alzheimer's A: National Institute on Aging-Alzheimer's Association guidelines for the neuropathologic assessment of Alzheimer's disease: a practical approach. Acta Neuropathol 2012, 123:1-11.
[74] Nelson PT, Lee EB, Cykowski MD, Alafuzoff I, Arfanakis K, Attems J, Brayne C, Corrada MM, Dugger BN, Flanagan ME, Ghetti B, Grinberg LT, Grossman M, Grothe MJ, Halliday GM, Hasegawa M, Hokkanen SRK, Hunter S, Jellinger K, Kawas CH, Keene CD, Kouri N, Kovacs GG, Leverenz JB, Latimer CS, Mackenzie IR, Mao Q, McAleese KE, Merrick R, Montine TJ, Murray ME, Myllykangas L, Nag S, Neltner JH, Newell KL, Rissman RA, Saito Y, Sajjadi SA, Schwetye KE, Teich AF, Thal DR, Tome SO, Troncoso JC, Wang SJ, White CL, 3rd, Wisniewski T, Yang HS, Schneider JA, Dickson DW, Neumann M: LATE-NC staging in routine neuropathologic diagnosis: an update. Acta Neuropathol 2023, 145:159-73.
[75] Latimer CS, Melief EJ, Ariza-Torres J, Howard K, Keen AR, Keene LM, Schantz AM, Sytsma TM, Wilson AM, Grabowski TJ, Darvas M, O'Connor KD, Nolan AL, Edlow BL, Mac Donald CL, Keene CD: Protocol for the Systematic Fixation, Circuit-Based Sampling, and Qualitative and Quantitative Neuropathological Analysis of Human Brain Tissue. Methods Mol Biol 2023, 2561:3-30.
[76] Hyman BT, Phelps CH, Beach TG, Bigio EH, Cairns NJ, Carrillo MC, Dickson DW, Duyckaerts C, Frosch MP, Masliah E, Mirra SS, Nelson PT, Schneider JA, Thal DR, Thies B, Trojanowski JQ, Vinters HV, Montine TJ: National Institute on Aging-Alzheimer's Association

guidelines for the neuropathologic assessment of Alzheimer's disease. Alzheimers Dement 2012, 8:1-13.
[77] Strohbehn SD: Examining the Association Between an Endolysosomal Polygenic Risk Score and Alzheimer's Disease. Institute for Public Health Genetics. Seattle, WA: University of Washington, 2023. p. 74.
[78] Rose SE, Williams CA, Hailey DW, Mishra S, Kirkland A, Keene CD, Garden GA, Jayadev S, Young JE: Advancements in high-resolution 3D microscopy analysis of endosomal morphology in postmortem Alzheimer's disease brains. Front Neurosci 2023, 17:1321680.
[79] de Groot CJ, Hulshof S, Hoozemans JJ, Veerhuis R: Establishment of microglial cell cultures derived from postmortem human adult brain tissue: immunophenotypical and functional characterization. Microsc Res Tech 2001, 54:34-9.
[80] Tirosh I, Izar B, Prakadan SM, Wadsworth MH, 2nd, Treacy D, Trombetta JJ, Rotem A, Rodman C, Lian C, Murphy G, Fallahi-Sichani M, Dutton-Regester K, Lin JR, Cohen O, Shah P, Lu D, Genshaft AS, Hughes TK, Ziegler CG, Kazer SW, Gaillard A, Kolb KE, Villani AC, Johannessen CM, Andreev AY, Van Allen EM, Bertagnolli M, Sorger PK, Sullivan RJ, Flaherty KT, Frederick DT, Jane-Valbuena J, Yoon CH, Rozenblatt-Rosen O, Shalek AK, Regev A, Garraway LA: Dissecting the multicellular ecosystem of metastatic melanoma by single-cell RNA-seq. Science 2016, 352:189-96.
[81] Braak H, Braak E: Neuropathological stageing of Alzheimer-related changes. Acta Neuropathol 1991, 82:239-59.
[82] Thal DR, Rub U, Orantes M, Braak H: Phases of A beta-deposition in the human brain and its relevance for the development of AD. Neurology 2002, 58:1791-800.